Article Type: Full Paper

Design, Synthesis and Anti-HIV-1 Evaluation of a Novel Series of 1,2,3,4-Tetrahydropyrimidine-5-carboxylic acid Derivatives

Saghi Sepehri,[a,b] Sepehr Soleymani,[c] Rezvan Zabihollahi,[c] Mohammad R. Aghasadeghi,[c] Mehdi Sadat,[c] Lotfollah Saghaie,[a] Hamid R. Memarian,[d] Afshin Fassihi[a,*]

[a]Department of Medicinal Chemistry, School of Pharmacy and Pharmaceutical Sciences, Isfahan University of Medical Sciences, 81746-73461, Isfahan, Iran

E-mail: fassihi@pharm.mui.ac.ir (A. Fassihi)

[b]Department of Medicinal Chemistry, School of Pharmacy, Ardabil University of Medical Sciences, Ardabil, 5618953141, Iran

[c]Department of Hepatitis and AIDS, Pasteur Institute of Iran, Tehran, Iran

[d]Department of Chemistry, Faculty of Sciences, University of Isfahan, 81746-73441 Isfahan, Iran

A series of tetrahydropyrimidine derivatives (**2a-l**) were designed, synthesized and screened for anti-HIV-1 properties based on the structures of HIV-1 gp41 binding site inhibitors, **NB-2** and **NB-64**. A computational study was performed to predict the pharmacodynamics, pharmacokinetics and drug-likeness features of the studied molecules. Docking studies revealed that the carboxylic acid group in the molecules forms salt bridges with either Lys574 or Arg579. Physiochemical properties (e.g. molecular weight, number of hydrogen bond donors, number of hydrogen bond acceptors and number of rotatable bonds) of the synthesized compounds confirmed and exhibited that these compounds were within the range set by Lipinski's rule of five. Compounds **2e** and **2k** with 4-chlorophenyl substituent and 4-methylphenyl group at C4 position of the tetrahydropyrimidine ring was the most potent one among the tested compounds. This suggests that these compounds may serve as leads for development of novel small-molecule HIV-1 inhibitors.

Keywords: Synthesis •Anti-HIV agents • Tetrahydropyrimidine derivatives • Gp41

Introduction

One of the possible targets in the treatment of HIV-1 infection lies in the early steps of viral life cycle, including the process of entry and fusion of viral membrane into the host cell membrane which is mediated by two glycoproteins, gp120 and gp41.[1]

The transmembrane subunit of HIV-1 envelope (Env) glycoprotein, gp41, plays an important role in viral fusion. HIV entry is a complex process and involves three separate steps: viral attachment, co-receptor binding and finally fusion.[2] This process begins with the binding of gp120 protein to the CD4 and chemokine co-receptors CXCR4 or CCR5. Consequently, these interactions induce a conformational change in gp41 from a pre-fusogenic form to a fusogenic six-helix bundle (6-HB) structure; thus, allowing the introduction of the viral genome into the host cell.[3-5] The gp41 ectodomain contains a transmembrane zone responsible for attachment to the host cell membrane, two heptad repeat regions which are N-terminal heptad repeats (NHR) and C-terminal heptad repeats (CHR). NHRs form a central trimeric coiled-coil while three helices of CHRs are packed in an anti-parallel fashion into the highly preserved hydrophobic grooves of the central trimeric coiled-coil to form a trimer of helical hairpins that makes up the six-helix bundle.[6]

Compounds with inhibitory activity on HIV-1 mediated membrane fusion may bind to the gp41 NHR and/or CHR regions and block the 6-HB formation.[7] Lately, several small molecule gp41 inhibitors have been developed as non-peptide small-molecule candidates. In this regard, various sets of chemical scaffolds have been proposed as gp41 inhibitors [8-19] amongst, two pyrrol derivatives, **NB-2** and **NB-64** (Figure **1**), were introduced as novel HIV-1 fusion inhibitors by high-throughput screening method in 2004. These compounds bind to the gp41 protein via ionic and hydrophobic interactions. These two pyrrole derivatives block the formation of the 6HB at low micromolar concentration.[10,20]

Some main structural similarities can be recognized between **NB-2** and **NB-64** as known gp-41 inhibitors and Biginelli-type tetrahydropyrimidines for anti-HIV-1 activity (Figure **1**).

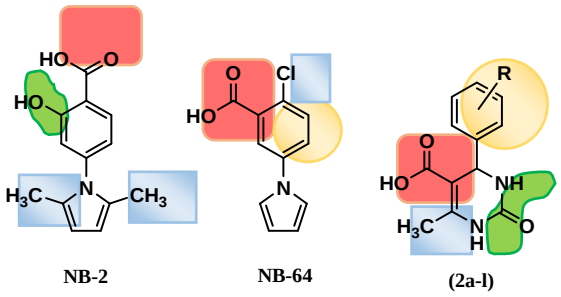

Figure 1. Carboxylic acid group is in red, hydrophobic moieties are shown inorange and blue. Hydrophilic groupsare represented in green

Most of the gp41 inhibitors such as **NB-2** and **NB-64** have a -COOH group in their scaffold to bind electrostatically to positively charged residues (Lys574 or Arg579) situated in the groove pocket. It is reported that the elimination of the -COOH group will decrease the anti-HIV-1 potency of the compound.[16] We have previously reported the moderate anti-HIV-1 activity of some Biginelli-type tetrahydropyrimidines (THPM, 6-methyl-2-oxo-4-aryl-1,2,3,4-tetrahydropyrimidine-5-carboxylate esters).[20] Tetrahydropyrimidines substituted with a carboxylic acid derivative at the 5 position have the proper functionality which is supposed to significantly influence the binding orientation, because it is predicted to form a salt bridge with Lys574 or Arg579 on the surface of the binding site (compounds **2a-l**, Figure **1**, shown in red squares). Aromatic rings, as hydrophobic moieties, have shown good interaction with the hydrophobic pocket of the gp41 active site and have improved the potency of inhibitors.[15] Substituted phenyl rings on the C-4 position of THPM ring could fulfill the interactions with the hydrophobic pocket located in the gp41 active site (compounds **2a-l**, Figure **1**, yellow circles). Some other hydrophobic groups in the THPM structure are able to interact with hydrophobic amino acids situated in the active site similar to the hydrophobic groups in **NB** compounds (compounds **2a-l**, Figure **1**, blue squares). An important structural aspect of **NB-2** and **NB-64** which is involved in the interaction with hydrophobic binding surface of the gp41 is the intersecting two-ring system consisted of pyrrol and substituted phenyl rings interconnected by a single bond. The two-ring molecular system of **NB** compounds has an analogue in tetrahydropyrimidine compounds: the substituted phenyl ring bisecting the tetrahydropyrimidine moiety. The possibility of hydrogen bonding increases the compound's potency.[15] Hydrogens attached to N-1 and N-3 of the THPM ring are assumed to take part in such hydrogen bonding with the hydrophilic amino acids (compounds **2a-l**, Figure **1**, green circles).

In this paper, in continuation of our previous report on the anti-HIV-1 activity of the Biginelli-type tetrahydropyrimidines, we describe the design, synthesis and HIV-1 inhibitory activity of a novel series of tetrahydropyrimidine analogues, 6-methyl-2-oxo-4-aryl-1,2,3,4-tetrahydropyrimidine-5-carboxylic acids. Intermolecular interactions of the studied compounds with the putative viral receptor, gp41, are also investigated in this research using molecular docking simulations.

Results and Discussion

Chemistry

The synthesis of 6-methyl-2-oxo-4-aryl-1,2,3,4-tetrahydropyrimidine-5-carboxylic acid derivatives (**2a-l**) was performed as outlined in Scheme **1**. Biginelli reaction between the corresponding aldehydes, benzyl 3-oxobutanoate and urea provided 6-methyl-2-oxo-4-aryl-1,2,3,4-tetrahydropyrimidine-5-carboxylate esters (**1a-l**). This reaction was performed in refluxing absolute ethanol in the presence of the catalytic amounts of $Co(HSO_4)_2$. Benzyl 3-oxobutanoate was prepared according to the modified method of Clemens via condensation of 2,2,6-trimethyl-1,3-dioxine-4-one with benzyl alcohol in refluxing xylene.[21] Catalytic transfer hydrogenation of **1a-l** in the presence of catalytic amounts of Pd/C (10% w/w) and ammonium formate in dry methanol yielded **2a-l** (Scheme **1**). Chemical structures were confirmed by ^{1}H-NMR, FT-IR, mass spectroscopy, and elemental analysis. FT-IR spectra of the final compounds exhibited characteristic absorption peaks for the ureide N-H bonds at 3102-3260 cm^{-1} and 3222-3396 cm^{-1}. A broad peak of carboxylic acid OH group and a signal of carboxylic acid C-O stretch band were observed at around 2500-3500 cm^{-1} and 1230-1290 cm^{-1}, respectively. Presence of carboxylic acid C=O group was confirmed by a strong absorption at 1686-1709 cm^{-1}. ^{1}H-NMR spectra revealed a broad singlet at 11.60-12.24 ppm demonstrating the existence of carboxylic acid group in the final compounds. The presence of the THPM ring was confirmed by two peaks in 8.85-9.75 ppm and 7.37-8.08 ppm belonging to ureide N-H bonds and a peak at 4.01-5.21 ppm attributable to the C-4 proton of the THPM ring. Other ^{1}H-NMR spectral signals were in accordance with the proposed structures.

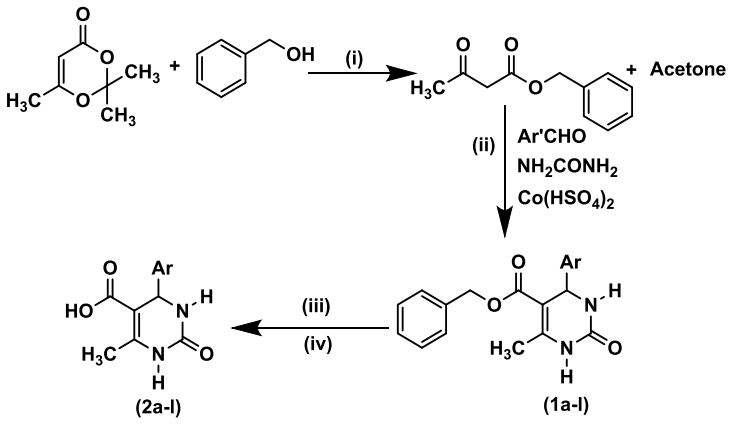

Scheme 1. Synthesis of compounds (**2a-l**). Reagents and conditions: (**i**) xylene, reflux, 3.5 h, (**ii**) EtOH, reflux, 24-48 h, (**iii**) MeOH, Pd/C (10%), HCO_2NH_4, room temperature, 24-48 h, (**iv**) NaOH 0.5 M, vigorously stirred then acidified by HCl 2 M to pH 4-5

Chemical structures of the prepared compounds are summarized in Table 1.

Table 1. General structure and structural details of the prepared compounds

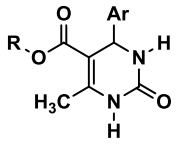

(1a-l) , (2a-l)

Compound	Ar	R	Mol. formula	Mol. weight
1a	Phenyl	$C_5H_6CH_2$	$C_{19}H_{18}N_2O_3$	322.36
1b	4-Dimethylaminophenyl	$C_5H_6CH_2$	$C_{21}H_{23}N_3O_3$	365.43
1c	4-Nitrophenyl	$C_5H_6CH_2$	$C_{19}H_{17}N_3O_5$	367.36
1d	2-Furyl	$C_5H_6CH_2$	$C_{17}H_{16}N_2O_4$	312.32
1e	4-Chlorophenyl	$C_5H_6CH_2$	$C_{19}H_{17}ClN_2O_3$	356.81
1f	4-Florophenyl	$C_5H_6CH_2$	$C_{19}H_{17}FN_2O_3$	340.35
1g	2-Chlorophenyl	$C_5H_6CH_2$	$C_{19}H_{17}ClN_2O_3$	356.81
1h	Styryl	$C_5H_6CH_2$	$C_{21}H_{20}N_2O_3$	348.40
1i	3-Nitrophenyl	$C_5H_6CH_2$	$C_{19}H_{17}N_3O_5$	367.36
1j	2-Thienyl	$C_5H_6CH_2$	$C_{17}H_{16}N_2O_3S$	328.39
1k	4-Methylphenyl	$C_5H_6CH_2$	$C_{20}H_{20}N_2O_3$	336.39
1l	2-Hydroxyphenyl	$C_5H_6CH_2$	$C_{19}H_{18}N_2O_4$	338.36

2a	Phenyl	H	$C_{12}H_{12}N_2O_3$	232.24
2b	4-Dimethylaminophenyl	H	$C_{14}H_{17}N_3O_3$	275.31
2c	4-Aminophenyl	H	$C_{12}H_{13}N_3O_3$	247.25
2d	2-Furyl	H	$C_{10}H_{10}N_2O_4$	222.20
2e	4-Chlorophenyl	H	$C_{12}H_{11}ClN_2O_3$	266.68
2f	4-Florophenyl	H	$C_{12}H_{11}FN_2O_3$	250.23
2g	2-Chlorophenyl	H	$C_{12}H_{11}ClN_2O_3$	266.68
2h	Styryl	H	$C_{14}H_{14}N_2O_3$	258.28
2i	3-Aminophenyl	H	$C_{12}H_{13}N_3O_3$	247.25
2j	2-Thienyl	H	$C_{10}H_{10}N_2O_3S$	238.27
2k	4-Methylphenyl	H	$C_{13}H_{14}N_2O_3$	246.27
2l	2-Hydroxyphenyl	H	$C_{12}H_{12}N_2O_4$	248.24

Biological assay

In this study, a series novel 1,2,3,4-THPM derivatives were synthesized and assessed for anti-HIV-1 activity in terms of inhibitory activity against HIV-1 replication in HEK cell cultures. All the synthesized molecules were also tested for their cytotoxicity on MT-2 cell line by XTT assay. The 5-carboxylate benzyl ester analogues (**1a-l**) were also subjected to both these assays.

The main focus of this study was to assess the HIV-1 growth inhibitory activity of 1,2,3,4-dihydropyrimidine-based compounds with the aim of finding important structural prerequisites for this property. The evaluated compounds did not exhibit significant cytotoxicity at concentration of 100 µM. Moderate HIV-1 replication inhibitory activities at 100 µM were recorded for the synthesized analogues. These results are summarized in Table **2**.

Compounds **1e**, **1i**, **2e** and **2k** were found to be the most potent anti-HIV-1 agents among the studied compounds, **1a-l** and **2a-l**. They had moderate HIV-1 replication inhibitory activity in range 42.6-52.3% at 100 µM.The other derivatives were less active. Moreover, almost all compounds displayed high cell viability. Compound **2k** showed the lowest cell viability among others (59.41% at 100 µM). It can be concluded from the data in Table **2** that the intermediate compounds **1a-l** were mostly weaker anti-HIV-1 agents and the inhibiting activity of **2a-l** series will be discussed as follows.

Molecules possessing phenyl and styryl groups at C4 position of THPM ring (**2a** and **2h**) showed lower activity compared to the other compounds bearing different substituents at this position. The inhibition values for **2e** and **2k** as the most potent compounds in **2a-l** series revealed that 4-chlorophenyl substituent at C4 position of 1,2,3,4-tetrahydropyrimidine (**2e**) was more favorable for HIV-1 inhibitory activity than 4-methylphenyl group (**2k**). Replacing 4-chlorophenyl ring with 4-flurophenyl decreased the activity. It seems that the higher lipophilicity character has constructive impacts on both hydrophobic interactions with receptor and virus accessibility, *i.e.*, host cell membrane permeability of the compounds. The lipophilicity feature of these compounds determined as CLogP by MolinspirationWebME Editor1.16. is supportive for this idea: CLogP for **2e** is 2.06 and for **2f** is 1.54.

Compound **2g** with 2-chlorophenyl substitution at C4 position of THPM exhibited lower anti-HIV-1 compared with compound **2e**, which has a 4-chlorophenyl derivative. An explanation for this difference is provided in the computational studies section.

Displacement of amino substitution from *meta* to *para* position diminished the activity. This will be explained in terms of ligand-gp41 interaction in the next section.

Replacement of 2-furyl moiety at C4 position of **2d** with 2-thienyl in **2j** decreased the activity.

Compound **2g** with 2-chlorophenyl at C4 position displayed better anti-HIV-1 activity compared to compound **2l** with 2-hydroxyphenyl moiety. This can be attributed to the better cell membrane permeation of **2g** cross the infected host cell to exert its anti-HIV-1 activity. This is in accordance with the differences between CLogP values of these compounds.

Table 2. Anti-HIV-1 activity of the prepared compounds

Compound	100 µM	
	(%) inhibition of P_{24} expression	(%) cell viability
1a	23.7± 1.2	93.7± 1.9
1b	5.7± 2.8	90.9± 1.7
1c	36.6± 3.7	100± 5.3
1d	22.5± 2.5	100± 5.3
1e	47.5± 2.5	100± 1.6
1f	4.7± 1.8	100± 1.8
1g	18.7± 3.7	97.14± 4.3
1h	0± 1.2	0± 4.4
1i	52.2± 1.2	69.0± 9.1
1j	0± 2.5	0± 5.1
1k	0±1.7	0±2.0
1l	0±2.5	0±4.1
2a	1.84± 1.2	100± 4.36
2b	35.1± 4.0	97.8± 1.4
2c	16.9± 1.6	100± 3.2
2d	41.2± 3.7	100± 5.3
2e	49.5± 2.5	98.9± 0.6
2f	28.8± 3.7	100± 5.06
2g	40.2± 1.2	76.7± 3.5
2h	4.5± 4.2	65.9± 10.1
2i	41.2±9.8	87.4± 2.1
2j	28.8± 3.7	70.7± 0.51

2k	42.6± 2.4	59.4± 1.2
2l	36.2± 3.7	75.1± 5.1
BMS-806	100	100

In silico studies

In silico calculation of physicochemical parameters and toxicity studies

As a part of our investigation, a computational study was performed for estimating drug-likeness and bioavailability of compounds. A prerequisite for any bioactive molecule to be developed as a therapeutic agent is good oral bioavailability.[22] Significant predictors of good oral bioavailability are good intestinal absorption, molecular flexibility (measured by the number of rotatable bonds (n-ROTB) and low polar surface area or total hydrogen bond count (sum of donors and acceptors).[22,23] Lipinski predicted the ''drug-likeness'' of potential molecular targets in formulating his "Rule of Five".[24] This rule states that most molecules with good membrane permeability should have partition coefficient values (logP) in the octanol-water system ≤ 5, molecular weight (MW) ≤ 500, number of hydrogen bond acceptors ≤ 10 and number of hydrogen bond donors ≤ 5. Drug-likeness can be assumed as a subtle balance between the molecular properties of a compound that directly influence its pharmacokinetics i.e. its absorption, distribution, metabolism, and excretion (ADME) in human body.[25] Numerical values for CLogP (calculated LogP), LogS (the logarithm of aqueous solubility in terms of mol/L), topological polar surface area (TPSA, a physicochemical property describing the polarity of molecules), number of H-bond donors, number of H-bond acceptors, and number of rotatable bonds are given in Tables **3** and **4**. TPSA is a key aspect in transport across membranes. It has been known as a good parameter for prediction of passive drug transport through membrane. It is validated by the good correlation of TPSA with published absorption data. These data are acquired from different kinds of drug absorbance, including human intestinal absorption, blood brain barrier crossing, and Caco-2 monolayer penetration.[26] Passively-absorbed molecules with a TPSA of greater than 140 $Å^2$ tend to be poor at permeating cell membranes; thus, they show low oral bioavailability.[26,27] Zhao *et al.* reported equation (**1**) that can predict the amount of oral drug absorption.[28]

$$\%ABS = 109 - (0.345 \times TPSA) \qquad \text{Eq. (1)}$$

All of the designed compounds in the present study possessed TPSA < 124 $Å^2$ and exhibited ABS > 66% (Table **4**). Thus, it seems that they could have a good capacity for penetrating cell membranes.

Our analysis of data depicted in Table **3** reveals that all of the synthesized derivatives had low MW, favorable CLogP, and favorable hydrogen bond-donating and acceptable capabilities. This in turn fits with the Lipinski's rule of five indicating that these compounds may have good absorption or permeability properties through the biological membranes. A low CLogP in the range of 0-3 is necessary to decrease the toxicity and increase the bioavailability for optimal oral absorption. All of the studied compounds had CLogP values within this range (Table **3**).

Solubility is another general physicochemical factor in drug discovery. An indication of the solubility of compounds is LogS value. The aqueous solubility of a compound remarkably influences its distribution and absorption characteristics. More than 80% of the drugs on the market have a logS value greater than -4 mol/L.[29] As shown in Table **4**, compounds **1c**, **1e**, **1g**, **1h** and **1i** had lower calculated solubility, less than -4 mol/L, whereas the rest of the compounds had higher calculated solubility, -1.90 to -3.98 mol/L.

Table 3. Calculated pharmacokinetic parameters for the prepared compounds

Compound	CLogP [a]	n-ROTB [b]	HBA [c]	HBD [d]	Volume [e]
1a	3.59	5	5	2	293.97
1b	3.69	6	6	2	339.88
1c	3.55	6	8	2	317.31
1d	2.85	5	6	2	275.54
1e	4.27	5	5	2	307.51
1f	3.75	5	5	2	298.90
1g	4.22	5	5	2	307.51
1h	4.35	6	5	2	321.39
1i	3.52	6	8	2	317.31
1j	3.49	5	5	2	284.69
1k	4.04	5	5	2	310.54
1l	3.53	5	6	3	301.99
2a	1.38	2	5	3	204.80
2b	1.48	3	6	3	250.70
2c	0.46	2	6	5	216.09
2d	0.64	2	6	3	186.37
2e	2.06	2	5	3	218.33
2f	1.54	2	5	3	209.73
2g	2.01	2	5	3	218.33

2h	2.13	3	5	3	232.21
2i	0.43	2	6	5	216.09
2j	1.28	2	5	3	195.51
2k	1.83	2	5	3	221.36
2l	1.32	2	6	4	212.81

[a]CLogP, logarithm of compound partition coefficient between n-octanol and water; [b]n-ROTB, number of rotatable bonds; [c]HBA, number of hydrogen bond acceptors; [d]HBD, number of hydrogen bond donors, [e]Å^3.

Lipinski's violations for all compounds were equal to 0.

Table 4. Prediction of the studied anti-HIV-1 compounds as drugs

Compound	LogS[a]	TPSA[b]	%ABS[c]	Drug-likeness	Drug-score[d]
1a	-3.67	67.43	85.73	-8.44	0.4
1b	-3.71	70.67	84.61	-9.22	0.24
1c	-4.31	113.25	69.93	-8.52	0.13
1d	-3.35	80.57	81.20	-8.71	0.43
1e	-4.41	67.43	85.73	-7.13	0.35
1f	-3.98	67.43	85.73	-8.83	0.39
1g	-4.41	67.43	85.73	-8.19	0.35
1h	-4.49	67.43	85.73	-9.78	0.35
1i	-4.31	113.25	69.93	-8.73	0.22

1j	-3.68	95.67	75.99	-7.07	0.41
1k	-4.01	67.43	85.73	-9.64	0.38
1l	-3.37	87.66	78.75	-8.62	0.42
2a	-2.22	78.43	81.94	3.41	0.93
2b	-2.26	81.67	80.82	2.50	0.54
2c	-2.30	124.25	66.13	3.55	0.93
2d	-1.90	91.57	77.41	3.16	0.94
2e	-2.95	78.43	81.94	4.70	0.90
2f	-2.53	78.43	81.94	2.98	0.91
2g	-2.95	78.43	81.94	3.57	0.89
2h	-3.04	78.43	81.94	2.03	0.85
2i	-2.86	124.25	66.13	-0.44	0.38
2j	-2.23	78.43	81.94	4.70	0.94
2k	-2.56	78.43	81.94	2.10	0.88
2l	-1.92	98.66	74.96	3.07	0.93

[a]Logarithm of aqueous solubility measured in M; [b] Topological polar surface area in Å^2;

[c]Percentage of Human oral absorption in GI; [d] Drug score combines drug likeness, CLogP, logS,

molecular weight and toxicity risks;

None were predicted mutagen exept for **1c**.

None were predicted tumorigen exept for **1b** and **2b**.

None were predicted irritant.

None were predicted to have reproductive effects except for **1c**, **1i** and **2i**.

Hydrogen-bonding ability has also been known as an important factor for describing drug permeability.[24,25] All the synthesized compounds possessed a satisfactory number of proton donor (≤ 5) and proton acceptor (≤ 8) groups to construct efficient interactions with the hydrophilic amino acids of the active site (Table **3**).

Decreased molecular flexibility measured by the number of rotatable bonds (optimally below 8) is another important predictor of good oral bioavailability.[22,23] According to analysis of data depicted in Table **3**, all of the synthesized derivatives had a low number of rotatable bonds (<5) as they obtain a high to moderate degree of structural rigidity.

Toxicity risk (mutagenicity, tumorogenicity, irritation, and reproductive effects) are signals alarming that the designed compounds may be harmful concerning the risk category specified. Most of the compounds did not show any potential of toxicity in toxicity risk assessment (Table**4**).

In Osiris calculations the drug-likeness prediction is a fragment-based approach. A positive drug-likeness value states that a molecule contains mainly fragments which are often present in commercial drugs. Osiris study displayed that compounds **2e** and **2j** had high positive drug-likeness values, and the fragments of these compounds had a contribution for drug-like activities. The drug-score prediction process in Osiris explorer depends on the combination of drug-likeness, CLogP, LogS, MW, and toxicity risks in one neat amount. This factor may be used to judge about the compound's overall potential as a qualified drug.[29] The studied compounds revealed moderate to good drug score introducing them as potentially safe lead compounds. Drug-likeness and drug-score values of the designed compounds are presented in Table **4**.

Molecular docking studies

Molecular docking simulations and analysis of the binding modes of the designed inhibitors within gp41 binding site were performed to rationalize the anti-HIV-1 activity results. AutoDock is a qualified docking program that has facilitated the process of drug design (The AutoDock Web site. http://autodock.scripps.edu).[30]

At the first step of docking, it was focused on the exploration of the binding mode of both **NB-2** and **NB-64** as potent gp41 inhibitors within the entire protein via a blind-docking procedure to validate the applied docking protocol. To get the detailed procedure, readers are referred to our previous report.[20] Then 1,2,3,4-THPM derivatives were docked into the binding site of gp41. All these compounds have a chiral center at the C-4 position of the tetrahydropyrimidine ring. Thus, both R and S enantiomers were considered in the molecular docking simulation studies. Docking results consisting of electrostatic, hydrophobic, hydrogen bonds, and predicted docking affinities of molecules are summarized in Tables **5-10**.

Table 5. Estimated hydrogen bonds for the bestdocked conformations (R-enantiomer)

Compound	Participant amino acid	Optimized hydrogen bond distances (Å)	Involved atom of the ligand	Involved atom of the amino acid
1a	Gln567	2.81	(THPM) N-3-H	C=O
1b	Gln567	2.75	(THPM) N-3-H	C=O
1c	Lys574	1.63	(Nitro) O	NH_3^+
1d	Gln567	2.74	(THPM) N-1-H	C=O
	Lys574	1.99	(Furyl) O	NH_3^+
1e	Gln567	2.35	(THPM) N-3-H	C=O
1f	Gln567	2.39	(THPM) N-3-H	C=O
1g	Gln567	1.88	(THPM) N-3-H	C=O
1h	Gln567	2.14	(THPM) N-1-H	C=O
1i	Lys574	2.68	(Nitro) O	NH_3^+
1j	Gln567	2.28	(THPM) N-3-H	C=O
1k	Gln567	2.79	(THPM) N-3-H	C=O
1l	Gln567	2.58	(Phenol) OH	C=O
2a	Gln567	1.78	(THPM) N-1-H	NH_2
	Lys574	2.03	(Acid) OH	C=O

	Gln567	2.11	(THPM) N-1-H	NH_2
2b				
	Lys574	1.95	(Acid) OH	C=O
	Lys574	2.87	(Acid) OH	C=O
2c				
	Gln575	2.78	(Carbonyl) O	NH_2
	Gln567	1.57	(THPM) N-1-H	NH_2
2d				
	Lys574	1.67	(Acid) OH	C=O
	Gln567	2.03	(THPM) N-1-H	NH_2
2e				
	Lys574	1.57	(Acid) OH	C=O
	Gln567	2.59	(THPM) N-1-H	NH_2
2f				
	Lys574	2.37	(Acid) OH	C=O
	Gln567	1.51	(THPM) N-1-H	NH_2
2g				
	Lys574	1.54	(Acid) OH	C=O
	Gln567	1.93	(THPM) N-1-H	NH_2
2h				
	Lys574	1.74	(Acid) OH	C=O
	Lys574	2.97	(Acid) OH	NH_3^+
2i				
	Gln567	2.31	(THPM) N-1-H	NH_2
	Gln567	1.98	(THPM) N-1-H	NH_2
2j				
	Lys574	1.82	(Acid) OH	C=O

	Gln567	2.12	(THPM) N-1-H	NH_2
2k				
	Lys574	2.02	(Acid) OH	C=O
	Gln567	2.12	(Phenol) OH	NH_2
2l	Lys574	1.79	(Acid) OH	C=O
	Gln575	1.84	(THPM) N-1-H	C=O
	Lys574	1.98	(Carbonyl) O	NH_3^+
BMS-806				
	Trp571	2.98	(Carbonyl) O	NH_2

Table 6. Estimated hydrogen bonds for the bestdocked conformations (S-enantiomer)

Compound	**Participant amino acid**	**Optimized hydrogen bond distances (Å)**	**Involved atom of the ligand**	**Involved atom of the amino acid**
1a	-	-	-	-
1b	Gln567	2.91	(THPM) N-3-H	C=O
1c	Lys574	1.63	(Nitro) O	NH_3^+
	Gln567	2.14	(THPM) N-1-H	C=O
1d				
	Lys574	1.99	(Furyl) O	NH_3^+
1e	Gln567	2.35	(THPM) N-3-H	C=O
1f	Gln567	2.39	(THPM) N-3-H	C=O

1g	Gln567	1.88	(THPM) N-3-H	C=O
1h	Gln567	2.25	(THPM) N-1-H	C=O
1i	Lys574	1.87	(Nitro) O	NH_3^+
1j	Gln567	2.34	(THPM) N-3-H	C=O
1k	Gln567	2.94	(THPM) N-3-H	C=O
1l	Gln567	2.78	(THPM) N-3-H	C=O
	Gln567	2.83	(Phenol) OH	C=O
2a	Gln567	1.85	(THPM) N-1-H	NH_2
	Lys574	1.96	(Acid) OH	C=O
2b	Gln567	2.00	(THPM) N-1-H	NH_2
	Lys574	1.78	(Acid) OH	C=O
2c	Gln575	2.32	(Carbonyl) O	NH_2
	Lys574	1.95	(Acid) OH	C=O
2d	Gln567	2.22	(THPM) N-1-H	NH_2
	Lys574	1.76	(Acid) OH	C=O
2e	Gln567	2.32	(THPM) N-1-H	NH_2
	Lys574	1.75	(Acid) OH	C=O
2f	Gln567	2.13	(THPM) N-1-H	NH_2

	Lys574	1.89	(Acid) OH	C=O
	Gln567	1.21	(THPM) N-1-H	NH_2
2g				
	Lys574	1.61	(Acid) OH	C=O
	Gln567	2.06	(THPM) N-1-H	NH_2
2h				
	Lys574	1.95	(Acid) OH	C=O
	Lys574	1.89	(Acid) OH	NH_3^+
2i				
	Gln567	2.03	(THPM) N-1-H	NH_2
	Gln567	2.57	(THPM) N-1-H	NH_2
2j				
	Lys574	2.05	(Acid) OH	C=O
	Gln567	1.83	(THPM) N-1-H	NH_2
2k				
	Lys574	1.55	(Acid) OH	C=O
	Gln567	2.43	(Phenol) OH	NH_2
2l	Lys574	1.43	(Acid) OH	C=O
	Gln575	2.21	(THPM) N-1-H	C=O
	Lys574	1.98	(Carbonyl) O	NH_3^+
BMS-806				
	Trp571	2.98	(Carbonyl) O	NH_2

Table 7. Estimated electrostatic, hydrophobic, π-π stacking and cation-π interactions for the best docked conformations (R-enantiomer)

Compound	Electrostatic interaction	Hydrophobic interaction	π-π Stacking interaction
1a	-	Lys574, Gln567, Trp571, Trp631, Val570, Gln575	**Trp571**
1b	-	Lys574, Gln567, Trp571, Gln575, Val570, Leu568, Trp631	**Trp571**
1c	Lys574	Lys574, Gln567, Trp571, Leu568, Trp631	Trp631
1d	-	Lys574, Gln567, Trp571, Leu568, Trp631, Val570	Trp571
1e	-	Lys574, Gln567, Trp571, Leu568, Trp631, Val570, Gln575	-
1f	-	Lys574, Gln567, Trp571, Leu568, Trp631, Val570, Gln575	-
1g	-	Gln567, Trp571, Leu568, Trp631, Val570, Glu634, Leu568, Glu630	-
1h	-	Lys574, Gln567, Trp571, Leu568, Trp631, Gln575	Trp571
1i	Lys574	Lys574, Gln567, Trp571, Glu630, Leu568, Trp631, Gln575, Glu634, Val570	Trp571
1j	-	Lys574, Gln567, Trp571, Glu630, Leu568, Trp631, Val570	-
1k	-	Lys574, Gln567, Trp571, Val570, Leu568, Trp631, Gln575	Trp631
1l	-	Lys574, Gln567, Trp571, Glu630, Leu568, Trp631, Val570	**-**
2a	Lys574	Lys574, Gln567, Trp571, Gln575, Val570	**-**
2b	Lys574	Lys574, Gln567, Trp571, Leu568	**-**
2c	Lys574	Lys574, Gln567, Trp571, Gln575, Val570	**-**

2d	Lys574	Lys574, Gln567, Trp571, Gln575, Val570	-
2e	Lys574	Lys574, Gln567, Trp571, Gln575, Val570	-
2f	Lys574	Lys574, Gln567, Trp571, Gln575, Val570	-
2g	Lys574	Lys574, Gln567, Trp571, Gln575, Val570	-
2h	Lys574	Lys574, Gln567, Trp571, Gln575, Val570	Trp571
2i	Lys574	Lys574, Gln567, Trp571, Gln575, Val570	-
2j	Lys574	Lys574, Gln567, Trp571, Gln575, Val570	-
2k	Lys574	Lys574, Gln567, Trp571, Gln575, Val570	-
2l	Lys574	Lys574, Gln567, Trp571, Gln575, Val570	-
BMS-806	-	Lys574, Gln567, Trp571, Leu568, Glu634, Trp631	-

Only compound **1l** showed cation- π interactions with Lys574.

Table 8. Estimated electrostatic, hydrophobic, π-π stacking and cation-π interactions for the best docked conformations (S-enantiomer)

Compound	Electrostatic interaction	Hydrophobic interaction	π-π Stacking interaction
1a	-	Glu634, Gln567, Trp571, Leu568, Trp631	**Trp571**
1b	-	Lys574, Gln567, Trp571, Gln575, Val570, Leu568, Trp631	**-**
1c	Lys574	Lys574, Gln567, Trp571, Leu568, Trp631, Val570, Glu630, Glu634	Trp631
1d	-	Lys574, Gln567, Trp571, Leu568, Trp631, Val570	Trp571
1e	-	Lys574, Gln567, Trp571, Glu634, Leu568, Trp631, Val570	-
1f	-	Lys574, Gln567, Trp571, Leu568, Trp631, Val570	Trp631
1g	-	Lys574, Gln567, Trp571, Glu630, Leu568, Trp631, Val570	-
1h	-	Lys574, Gln567, Trp571, Val570, Leu568, Trp631, Gln575	**-**
1i	Lys574	Lys574, Gln567, Trp571, Glu630, Leu568, Trp631	-
1j	-	Lys574, Gln567, Trp571, Gln575, Leu568, Trp631, Val570	Trp571
1k	-	Lys574, Gln567, Trp571, Leu568, Trp631	-
1l	-	Lys574, Gln567, Trp571, Leu568, Trp631	**-**
2a	Lys574	Lys574, Gln567, Trp571, Gln575, Val570	**-**
2b	Lys574	Lys574, Gln567, Trp571, Gln575, Val570	**-**
2c	Lys574	Lys574, Gln567, Trp571, Gln575, Val570	**-**

2d	Lys574	Lys574, Gln567, Trp571, Gln575, Val570	-
2e	Lys574	Lys574, Gln567, Trp571, Gln575, Val570	-
2f	Lys574	Lys574, Gln567, Trp571, Gln575, Val570	-
2g	Lys574	Lys574, Gln567, Trp571, Gln575, Val570	-
2h	Lys574	Lys574, Gln567, Trp571, Gln575, Val570	Trp571
2i	Lys574	Lys574, Gln567, Trp571, Gln575, Val570	-
2j	Lys574	Lys574, Gln567, Trp571, Gln575, Val570	-
2k	Lys574	Lys574, Gln567, Trp571, Gln575, Val570	-
2l	Lys574	Lys574, Gln567, Trp571, Gln575, Val570	-
BMS-806	-	Lys574, Gln567, Trp571, Leu568, Glu634, Trp631	-

Only compounds **1f**, **1k** and **1l** showed cation- π interactions with Lys574.

Table 9. Docking energy results for the best docked conformations (S-enantiomer) docked into the fusion HIV-1 virus target

(gp41, PDB ID: 1AIK)

Compound	$\Delta G_{binding}$ (kcal/mol)	Intermol energy (kcal/mol)	Electrostatic energy (kcal/mol)	Vdw_hb_desolv energy (kal/mol)
1a	-5.94	-6.70	-0.58	-6.12
1b	-6.31	-7.32	-0.10	-7.21
1c	-6.71	-8.35	-2.15	-6.20
1d	-5.75	-6.69	-0.11	-6.57
1e	-6.25	-7.32	-0.39	-6.93
1f	-5.85	-7.03	-0.30	-6.74
1g	-5.89	-7.05	-0.41	-6.64
1h	-6.33	-7.46	-0.19	-7.27
1i	-6.97	-8.39	-1.91	-6.48
1j	-5.76	-6.94	-0.14	-6.80
1k	-6.17	-7.16	-0.22	-6.95
1l	-6.48	-7.62	-0.48	-7.14
2a	-5.31	-6.11	-0.12	5.87
2b	-5.45	-6.02	-1.63	-4.40

2c	-5.15	-5.73	-1.71	-4.02
2d	-4.48	-5.39	-1.29	-4.11
2e	-5.50	-6.03	-1.52	-4.51
2f	-5.31	-5.74	-1.62	-4.12
2g	-5.14	-5.91	-1.72	-4.19
2h	-5.38	-6.31	-1.56	-4.75
2i	-5.25	-6.16	-1.20	-4.97
2j	-4.85	-5.44	-1.17	-4.27
2k	-5.68	-5.90	-1.61	-4.29
2l	-5.23	-5.81	-1.34	-4.47
BMS-806	-6.42	-7.61	-0.19	-7.42

Table 10. Docking energy results for the best docked conformations (R-enantiomer) docked into the fusion HIV-1 virus target

(gp41, PDB ID: 1AIK)

Compound	**$\Delta G_{binding}$ (kcal/mol)**	**Intermol energy (kcal/mol)**	**Electrostatic energy (kcal/mol)**	**Vdw_hb_desolv energy (kal/mol)**
1a	-5.79	-7.02	-0.06	-6.97

1b	-6.23	-7.23	-0.04	-7.19
1c	-6.92	-8.24	-2.13	-6.11
1d	-5.48	-6.63	-0.24	-6.39
1e	-6.02	-7.37	-0.06	-7.31
1f	-5.64	-7.05	-0.10	-6.95
1g	-5.72	-7.03	-0.48	-6.54
1h	-6.55	-7.53	-0.05	-7.48
1i	-7.05	-8.69	-1.89	-6.79
1j	-5.52	-6.98	-0.39	-6.58
1k	-5.91	-7.23	-0.03	-7.20
1l	-6.87	-7.38	-0.30	-7.08
2a	-4.87	-5.58	-0.04	-4.73
2b	-5.19	-5.65	-1.29	-4.36
2c	-4.58	-5.61	-1.38	-4.23
2d	-4.36	-5.45	-1.68	-3.77
2e	-5.33	-5.60	-1.14	-4.46
2f	-4.84	-5.26	-1.54	-3.73
2g	-4.55	-5.49	-1.15	-4.33

2h	-5.01	-6.33	-1.39	-4.95
2i	-4.79	-6.01	-1.55	-4.46
2j	-4.43	-5.69	-1.70	-3.99
2k	-5.39	-5.49	-1.53	-3.96
2l	-4.64	-5.68	-1.78	-3.91
BMS-806	-6.42	-7.61	-0.19	-7.42

No significant differences were observed between the $\Delta G_{binding}$ of the R and S enantiomers of the intermediate compounds, **1a-l**. The interaction modes of the two enantiomers were almost the same with some minor exeptions. The greatest differences were as follows: S enantiomer of **1a** unlike the R enantiomer did not participate in hydrogen bonds with the gp41 receptor. R enantiomers of **1b**, **1f** and **1j**, and S enantiomer of **1i** and **1k** exhibited no π-π interactions with the receptor while the other enantiomers of these compounds were involved in such interactions. No cation-π interactions were observed for the R enantiomer of **1f** and **1k** unlike the S enantiomers of the compounds. The rest of the differences were some minor ones in type of the gp41 residues involved in the hydrophobic interactions. For the final compounds, **2a-l**, not only the $\Delta G_{binding}$ but also the interaction modes of the R and S enantiomers with the gp41 binding site were almost similar.

Analysis of the results of molecular docking studies revealed them to be almost confirming of the biological activity results. The most potent compound (**2e**) had an inhibition percentage equal to 49.50 in 100 µM. Docking studies demonstrated that **2e** participates in key interactions with gp41 binding site residues: an electrostatic contact with Lys574 and an H-bond with Gln567. Detailed analysis of hydrophobic binding patterns showed that an interaction exists between methyl group of 1,2,3,4-THPM ring and Val570. Moreover, 4-chlorophenyl substituent of the C-4 position is responsible for further hydrophobic interactions with Trp571, Gln575 and Lys574 in the hydrophobic pocket. Replacement of the methyl substituent in compound **2e** with Cl produced compound **2k** which was the most active final compound after **2e**. This compound contributes in H-bond and electrostatic contact with Gln567 and Lys574, respectively. Furthermore, investigating hydrophobic binding patterns showed that these interactions occurred between **2k** and Trp571, Gln575 and Val570 residues. Interactions of **2e** and **2k** with the binding site amino acids are shown in Figure **2**.

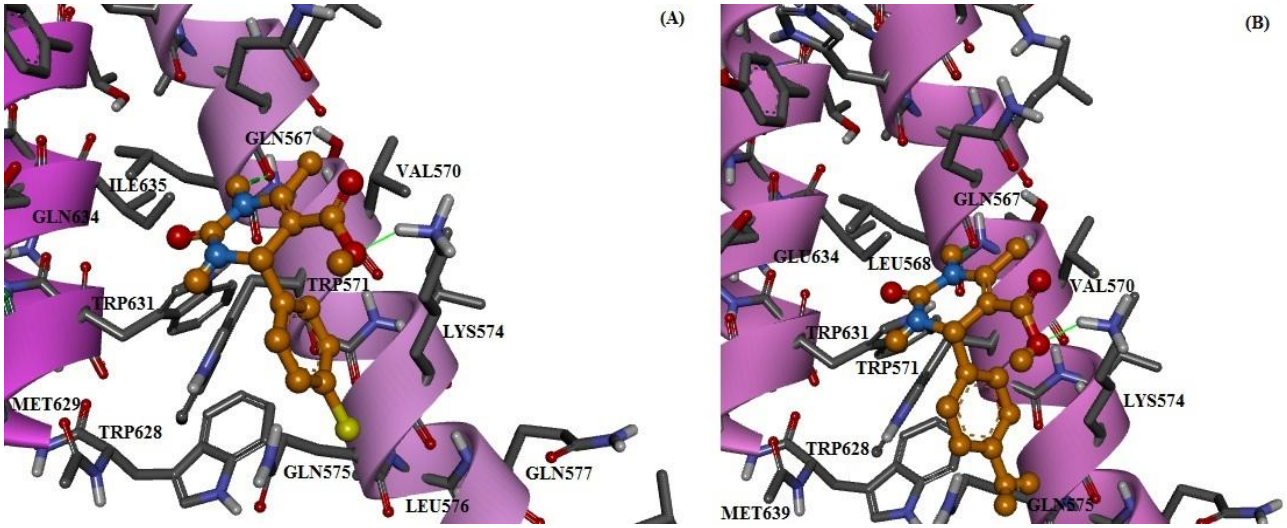

Figure 2. Docked conformations of **2e** S-enantiomer (**A**) and **2k** S-enantiomer (**B**) in the gp41 hydrophobic cavity showing possible interactions with the neighboring hydrophobic residues and Lys574.

As it was mentioned earlier, molecules possessing phenyl and styryl groups at C-4 position of THPM ring (**2a** and **2h**) showed lower activity (Table **2**). The lower anti HIV-1 activity of **2h** might be attributed to the improper geometric orientation of styryl group in the binding site of gp41. This can be seen in Figure **3** by superimposing **2h** and **2e** (the most active compound of the series) in the gp41 binding site.

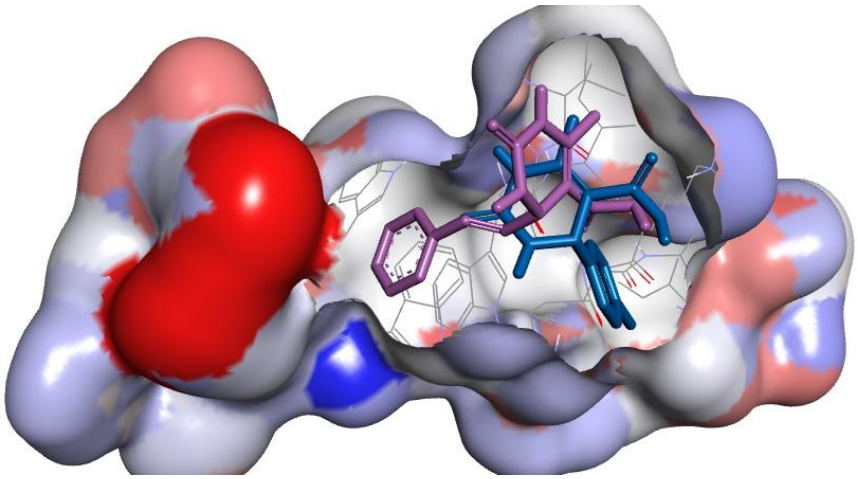

Figure 3. Superimposition of **2e** S-enantiomer (blue sticks) and **2h** S-enantiomer (violet sticks) from docking results in gp41 binding site

4-Chlorophenyl aromatic group at the C-4 position of 1,2,3,4-THPM ring in **2e** provided a more potent compound compared to 2-chlorophenyl substituent in **2g**. The docking results were supportive of this observation (Figure **4**). In fact, the binding mode of compound **2g** showed that the intermolecular interactions of the *ortho*-Cl with the neighboring residues were fewer compared with *meta*-Cl. This can be attributed to a steric hindrance leading to a change in the orientation of 2-chlorophenyl moiety of **2g** and subsequent weak interactions.

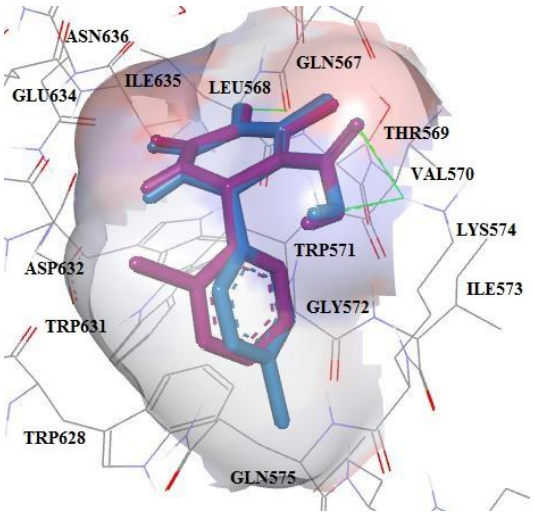

Figure 4. The superimposition of **2e** S-enantiomer (blue) with **2g** S-enantiomer (violet) in gp41 groove

Replacement of 4-chlorophenyl at C4 position of 1,2,3,4-THPM ring in **2e** with 4-flurophenyl in **2f** decreased the activity. According to the CLogP data, **2e** is more lipophilic than **2f**. Furthermore, the molecular volume of **2e** is more than **2f** (218.33 $Å^3$ and 209.73 $Å^3$, respectively), thus compound **2e** would occupy a larger space in the hydrophobic pocket and show better anti-HIV-1 activity.

Replacing 2-chlorophenyl (**2g**) with 2-hydroxyphenyl ring (**2l**) at the C-4 position of 1,2,3,4-THPM decreased the activity. Based on the previous researches, analogues with increased hydrophilic character were equal or slightly improved in potency, but addition of polar groups had a negative effect.[14] Thus, 2-chlorophenyl group provided additional hydrophobic contacts to residues at binding site. Moreover, docking results revealed that compound **2l** formed H-bonds with Gln567, Gln575 and Lys574, while compound **2g** participated in hydrogen bonding to Gln567 and Lys574 (Figure **5**).

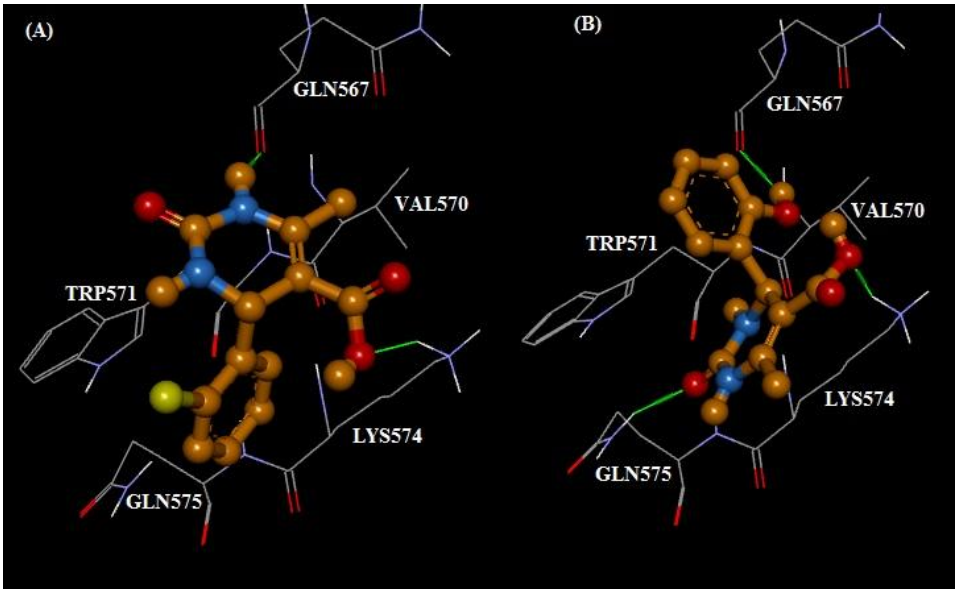

Figure 5. H-bonds and hydrophobic interactions of **2g** S-enantiomer (**A**) and **2l** S-enantiomer (**B**) in gp41 binding site

Compound **2b** with 4-dimethyaminophenyl showed higher activity than **2c** with 4-amine phenyl group. It seemed that due to existence of a bulk group at C4 position of **2b**, this compound has a bigger volume than **2c** (250.70 $Å^3$ for **2b** and 216.09 $Å^3$ for **2c**); thus **2b** would occupy more space in the hydrophobic pocket thus shows better anti-HIV-1 activity.

Compound **2c** with an amino group at *para* position of phenyl ring of C4 showed weaker activity than **2i** having amino group at *meta* position. According to the docking results, amine group at the meta position in **2i** forms H-bond with Gln567 residue but amine group at *para* position in **2c** does not form any H-bonds with this residue.

Compound **1i** had the most negative $\Delta G_{binding}$ value compared with other compounds. Thus, this molecule binds firmly to the receptor. It is obvious from its molecular structure that electrostatic interactions with the receptor are responsible for this. A nitro group shares electrostatic interaction with the positively charged residue Lys574. Moreover, this compound shows the highest activity compared with other compounds (52.25% inhibition at 100 µM) in series **1a-l**. It is accepted that the presence of a *meta* carboxylate group on N-substituted pyrrol ring of gp41 inhibitors favors the receptor interaction.[10] The *meta* nitro group on the phenyl ring located at the C4 position in **1i** takes part in the same electrostatic interaction with gp41 binding site. The *para* nitro analogue (**1c**) has a higher $\Delta G_{binding}$ value and a lower electrostatic contribution than **1i**. This may account for the differences between the anti-HIV potency of these compounds.

Ligand-residue binding energies and docked poses indicated that compound **2h** might participate in favorable π-π stacking contacts with Trp571. Nearly parallel orientation of aromatic rings (Trp571 indol ring and ligand phenyl ring) might be responsible for the detected π-π stacking interaction (Figure **6**).

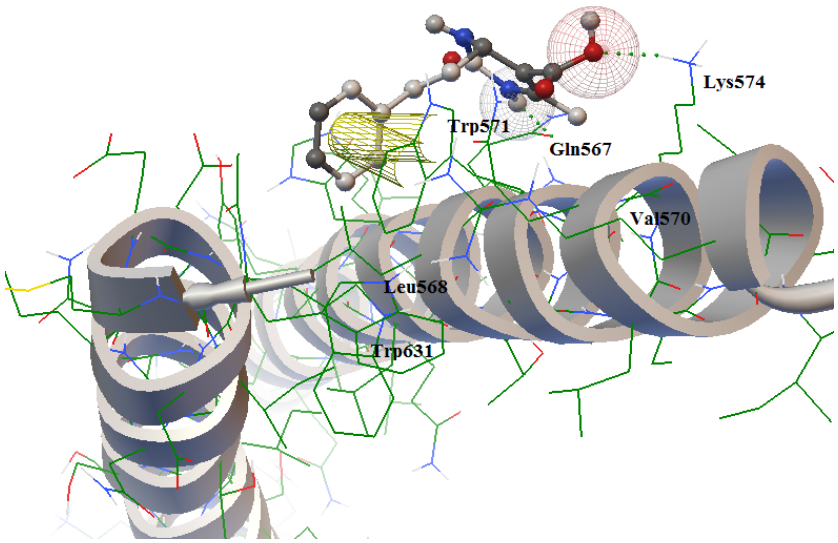

Figure 6. Nearly parallel orientation of **2h** S-enantiomer phenyl and Trp571 indol rings and possible π-π stacking interaction

All of the **2a-l** compounds participated in electrostatic interactions with Lys574 via their C-5-COOH group and most of them took part in hydrophobic interactions with Val570 via their C-6 methyl groups.

BMS-806 and related compounds are low-molecular-weight inhibitors of HIV-1 entry and attachment (the first steps of HIV-1 infection) that were identified by a viral infection-based screen. **BMS-806** was shown to be specific for HIV-1, with no activity against HIV-2 or simian immunodeficiency virus.[31] This compound as the control HIV-1 glycoprotein inhibitor was used in this the work. Compound **BMS-806** was docked into the gp41 binding site and showed interactions almost similar to **NB-2** and the synthesized derivatives. This compound formed H-bonds with Lys574 and Trp571. It was not able to interact electrostatically with the receptor since it lacks the proper functionalities (Figure **7**).

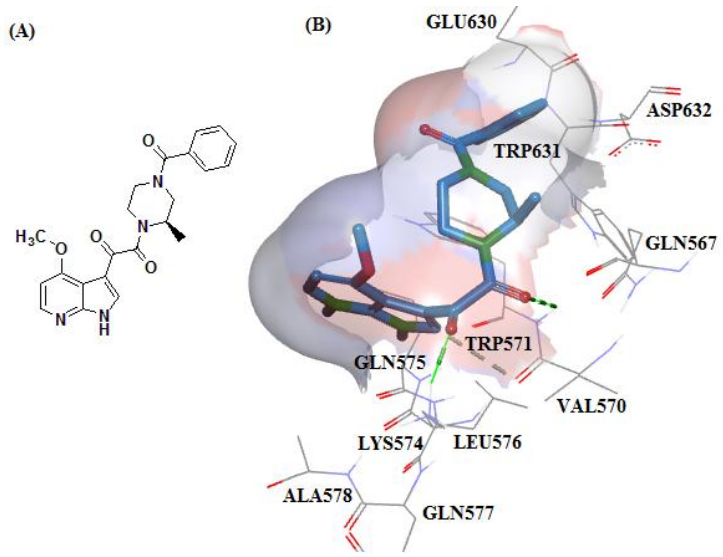

Figure 7. (A) Chemical structure of **BMS-806**, **(B) BMS-806** at the gp41 binding site

Finally, compounds **2e** and **2k** which were the most potent compounds in anti HIV-1 assay exhibited the highest $\Delta G_{binding}$ in the docking studies. Compound **2e** showed high cell viability (98.88% at 100 µM) and high positive drug-likeness values also. Compounds **2a**, **2c**, **2d** and **2f** did not show any cytotoxicity.

Conclusions

The synthesis procedure, structural characterization and anti-HIV-1 evaluation of a novel series of tetrahydropyrimidine analogues were provided in the present report. All analogues exhibited moderate to good anti-HIV-1 activity. Among these series, compounds **2e** and **2k** have shown the highest activity as an anti-HIV-1 agent. Structure-activity relationships analysis revealed that the presence of 4-chlorophenyl and 4-methylphenyl substituents at the C4 position of 1,2,3,4-THPM ring enhances the anti-HIV-1 activity and lowers the cytotoxic effect on MT-2 cell line. All of the compounds obeyed the Lipinski's "rule of five" and showed drug-likeness in terms of their ADMET profiles.

Molecular docking simulations were carried out to understand the effects of substituents on the anti-HIV-1 activity more. Molecular docking studies demonstrated the binding modes of this series into gp41 and also indicated the favorable interactions of the active molecules with the receptor residues. Based on these results we believe the present research would lead to the development of more potent anti-HIV-1 compounds.

Experimental Section

Chemistry

All of the reagents were purchased from commercial sources and were freshly used after being purified by standard procedures. Melting points were determined on the Electrothermal 9200 Melting Point apparatus and were uncorrected. ^{1}H-NMR spectrum was recorded in DMSO-d_6 on a Bruker-Ultrashield 400MHz spectrometer (Germany). All the chemical shifts are reported as (δ) values (ppm) against tetramethylsilane as an internal standard. Electrospray mass spectra (ESI-MS) were obtained in negative and positive ion mode on a SHIMADZU LCMS-2010 EV spectrometer using methanol as solvent, a capillary voltage of 4500 V and a cone voltage of 10 V. FT-IR and IR (KBr) spectra were recorded on JASCO 6300 (Japan) and Perkin-Elmer 1420 (USA) apparatus, respectively. All chemical reactions were monitored by analytical thin layer chromatography (TLC) on pre-coated silica gel 60 F254 aluminum plates (Merck, Germany). Suitable names for all the novel compounds were given with the aim of ChemOffice2010. Their purity was determined by thin layer chromatography using several solvent systems of different polarities and data obtained from elemental analysis, to an accuracy of within ±0.4%.

*General procedure for the synthesis of 6-methyl-2-oxo-4-aryl-1,2,3,4-tetrahydropyrimidine-5-carboxylate esters (**1a-l**)*

A combination of the proper aldehyde (3 mmol), benzyl 3-oxobutanoate (3.6 mmol), urea (3.9 mmol) and $Co(HSO_4)_2$ (0.6 mmol) in absolute ethanol (4 mL) was heated and stirred under reflux until the end of the reaction. The progress of the reaction was detected by TLC. After the completion of the reaction, the mixture was cooled to room temperature and crushed ice and water were added. Stirring continued for several minutes for dissolving the catalyst and the excess of urea. Solid products were filtered and washed with water. Pure products were obtained by recrystallization from ethanol. This procedure was performed for compounds **1a-1g** and **1i**, **1j**. For the rest of the compounds the process of purification was different: after completion of the reaction and addition of crushed ice and water, product was extracted with ethyl acetate or dichloromethane (10 mL × 3). The organic solvent was combined, dried over anhydrous Mg_2SO_4, filtered, and then evaporated. Pure products were obtained by recrystallization from ethanol. The obtained product was completely dried in a vacuum oven. General procedure for the preparation of these compounds is outlined in Scheme **1**.

*Benzyl 6-methyl-2-oxo-4-phenyl-1,2,3,4-tetrahydropyrimidine-5-carboxylate (**1a**)*

Synthesis and the structural features of this compound have been reported previously.[32]

*Benzyl 6-methyl-2-oxo-4-(4-(dimethylaminophenyl)-1,2,3,4-tetrahydropyrimidine-5-carboxylate (**1b**).*

Pale green precipitates. Yield: 85%.M.p. 195-196 °C.IR (KBr): 3364, 3291 (N-H, ureide), 3118 (C-H, aromatic), 2960 (C-H, aliphatic), 1699 (C=O, ester), 1521, 1452 (C=C, aromatic), 1216 (C-O, ester). ^{1}H-NMR (400 MHz, (D_6)DMSO): 9.16 (s, N-H(1): ureide), 7.61 (d, ^3J= 3.2, N-H(3): ureide), 7.28-7.29 (m, H-C(3), H-C(4), H-C(5): -$CH_2C_6H_5$), 7.15-7.16 (m, H-C(2), H-C(6): -$CH_2C_6H_5$), 7.02 (d, ^3J(H,H) = 8.4, H-C(2), H-C(6): -$C_6H_4N(CH_3)_2$), 6.64 (d, ^3J(H,H) = 8.8, H-C(3), H-C(5): -$C_6H_4N(CH_3)_2$), 5.07 (brs, H-C(4): THPM), 5.02 (m, H-C(1), H-C(2): $CH_2C_5H_6$), 2.86 (s, H-CH_3(N), , H-CH_3(N): -$C_6H_4N(CH_3)_2$), 2.25 (s, CH_3 -C(6): THPM).

*Benzyl 6-methyl-2-oxo-4-(4-nitrophenyl)-1,2,3,4-tetrahydropyrimidine-5-carboxylate (**1c**).*

White crystals. Yield: 87%. M.p. 172-173 °C. IR (KBr): 3354, 3224 (N-H, ureide), 3111 (C-H, aromatic), 2968 (C-H, aliphatic), 1693 (C=O, ester), 1633, 1446, 1427 (C=C, aromatic), 1064 (C-O, ester). ^{1}H-NMR (400 MHz, (D_6)DMSO): 9.42 (s, H-N(1): ureide), 8.16 (d, ^3J(H,H) = 8.8, H-C(3), H-C(5): -$C_6H_4NO_2$), 7.91 (brs, H-N(3): ureide), 7.46 (d, ^3J(H,H) = 8.8, H-C(2), H-C(6): -$C_6H_4NO_2$), 7.27-7.28 (m, H-C(3), H-C(4), H-C(5): -$CH_2C_6H_5$), 7.14-7.16 (m, H-C(2), H-C(6): -$CH_2C_6H_5$), 5.30 (brs, H-C(4): THPM), 5.20 (d, ^3J= 12.4, H-C(a): -$CH_2C_6H_5$), 5.00 (d, ^3J = 12.4, H-C(b): -$CH_2C_6H_5$), 2.29 (s, CH_3 -C(6): THPM).

*Benzyl 6-methyl-2-oxo-4-(furan-2-yl)-1,2,3,4-tetrahydropyrimidine-5-carboxylate (**1d**).*

White precipitates. Yield:71%.M.p. 192-193 °C.IR (KBr): 3368 & 3234 (N-H, ureide), 3121 (C-H, aromatic), 2974 (C-H, aliphatic), 1698 (C=O, ester), 1637, 1451 (C=C, aromatic), 1218 (C-O, ester). ^{1}H-NMR (400 MHz, (D_6)DMSO): 9.32 (s, H-N(1): ureide), 7.79 (d, ^3J= 3.2, H-N(3): ureide), 7.56 (brd, ^3J= 1.6, H-C(3): furan), 7.36-7.23 (m, H-C: -$CH_2C_6H_5$), 6.36 (dd, ^3J= 3.2, ^3J= 2.0, H-C(4): furan), 6.06 (d, ^3J= 3.2, H-C(5): furan), 5.25 (brs, H-C(4): THPM), 5.10 (d, ^3J= 12.8, H-C(a), -$CH_2C_6H_5$), 5.04 (d, ^3J= 12.8, H-C(b): -$CH_2C_6H_5$), 2.25 (s, CH_3 -C(6): THPM).

*Benzyl 6-methyl-2-oxo-4-(4-chlorophenyl)-1,2,3,4-tetrahydropyrimidine-5-carboxylate (**1e**).*

White crystals. Yield. 78%.M.p. 176-177 °C. IR (KBr): 3339, 3189 (N-H, ureide), 2973 (C-H, aliphatic), 1664 (C=O, ester), 1569, 1443 (C=C, aromatic), 1170 (C-O, ester).^{1}H-NMR (400 MHz, (D_6)DMSO):9.31 (s, H-N(1): ureide), 7.79 (d, ^3J= 3.6, H-N(3): ureide), 7.38-7.13 (m, H-C: -$CH_2C_6H_5$, -C_6H_4Cl), 5.17 (brs, H-C(4): THPM), 5.07 (d, ^3J= 12.8, H-C(a): $CH_2C_5H_6$), 4.99 (d, ^3J= 12.8, H-C(b): $CH_2C_5H_6$), 2.27 (s, CH_3 -C(6): THPM).

*Benzyl 6-methyl-2-oxo-4-(4-fluorophenyl)-1,2,3,4-tetrahydropyrimidine-5-carboxylate (**1f**).*

White crystals. Yield:81%.M.p. 181-182 °C.IR (KBr): 3354, 3225 (N-H, ureide), 3111 (C-H, aromatic), 2968 (C-H, aliphatic), 1694 (C=O, ester), 1633, 1447, 1415 (C=C, aromatic), 1216 (C-O, ester).^{1}H-NMR (400 MHz, (D_6)DMSO): 9.29 (s, H-N(1): ureide), 7.77 (d, ^3J= 3.2, H-N(3): ureide), 7.30-7.10 (m, H-C: -

$CH_2C_6H_5$, -C6H4F), 5.18 (brs, H-C(4): THPM), 5.07 (d, ^3J= 12.8, H-C(a): $CH_2C_5H_6$), 4.99 (d, ^3J= 12.8, H-C(b): $CH_2C_5H_6$), 2.27 (s, CH_3-C(6): THPM).

*Benzyl 6-methyl-2-oxo-4-(2-chlorophenyl)-1,2,3,4-tetrahydropyrimidine-5-carboxylate (**1g**).*

White crystals. Yield: 68%. M.p. 169-170 °C.IR (KBr): 3332, 3199 (N-H, ureide), 1664 (C=O, ester), 1568 (C=O, ureide), 1441 (C=C, aromatic), 1178 (C-O, ester), 851 (C-Cl, chlorine). ^{1}H-NMR (400 MHz, (D_6)DMSO):9.35 (s, H-N(1): ureide), 7.73 (d, ^3J= 3.2, H-N(3): ureide), 7.40-6.98 (m, H-C: -$CH_2C_6H_5$, -C_6H_4Cl), 5.67 (brs, H-C(4): THPM), 5.00 (d, ^3J= 12.8, H-C(a): $CH_2C_5H_6$), 4.93 (d, ^3J=12.8, H-C(b): $CH_2C_5H_6$), 2.32 (s, CH_3-C(6): THPM).

*(E)-Benzyl 6-methyl-2-oxo-4-styryl-1,2,3,4-tetrahydropyrimidine-5-carboxylate (**1h**).*

White precipitates. Yield 56%. M.p. 192-193 °C.IR (KBr): 3242.01, 3099.78 (N-H, ureide), 2945.59 (C-H, aliphatic), 1696.63 (C=O, ester), 1518.50, 1449.90 (C=C, aromatic), 1219.89 (C-O, ester). ^{1}H-NMR (400 MHz, (D_6)DMSO): 9.22 (s, H-N(3): ureide), 7.56 (s, H-N(1): ureide), 7.20-7.40 (m, H-C: -$CH_2C_6H_5$, -C_6H_5), 6.25-6.39 (d, ^3J= 16, H-C(b): $H_aC{=}CH_bC_6H_5$), 6.12-6.25 (m, H-C(a): $H_aC{=}CH_bC_6H_5$), 5.00-5.25 (d, ^3J = 12.6: $CH_2C_5H_6$), 4.76 (brs, H-C(4): THPM), 2.22 (s, CH_3-C(6): THPM).Mass m/z (%): 348.00 (M).

*Benzyl 6-methyl-2-oxo-4-(3-nitrophenyl)-1,2,3,4-tetrahydropyrimidine-5-carboxylate (**1i**).*

White crystals. Yield: 45%. M.p. 193-194 °C.IR (KBr): 3327, 3284 (N-H, ureide), 2953 (C-H, aliphatic), 1663 (C=O, ester), 1609, 1556, 1516 (C=C, aromatic), 1172 (C-O, ester).^{1}H-NMR (400 MHz, (D_6)DMSO):9.43 (s, H-N(1): ureide), 8.14 (s, H-N(3): ureide), 8.00 (s, H-C(2): -$C_6H_4NO_2$), 7.67-7.59 (m, H-C: -$CH_2C_6H_5$), 7.26-7.25 (m, H-C(4), H-C(5): -$C_6H_4NO_2$), 7.14-7.12 (m, H-C(6): -$C_6H_4NO_2$), 5.32 (brs, H-C(4): THPM), 5.08 (d, ^3J= 12.4, H-C(a): $CH_aC_5H_6$), 4.97 (d, ^3J = 12.4,H-C(b): $CH_bC_5H_6$), (s, CH_3-C(6): THPM).

*Benzyl 6-methyl-2-oxo-4-(thiophen-2-yl)-1,2,3,4-tetrahydropyrimidine-5-carboxylate (**1j**).*

White crystals. Yield: 73%. Mp. 162-163 °C.IR (KBr): 3350, 3202 (N-H, ureide), 2945 (C-H, aliphatic), 1667 (C=O, ester), 1570, 1444 (C=C, aromatic), 1195 (C-O, ester). ^{1}H-NMR (400 MHz, (D_6)DMSO):9.39 (s, H-N(1): ureide), 7.92 (d, ^3J = 3.6, H-N(3): ureide), 7.37-7.24 (m, H-C: -$CH_2C_6H_5$), 6.93 (dd, ^3J = 3.6,^3J = 3.6, H-C(4), H-C(5): thiophen), 6.86 (d, ^3J = 3.6, H-C(3): thiophen), 5.45 (brs, H-C(4): THPM), 5.10 (brs: $CH_2C_5H_6$), 2.25 (s, CH_3-C(6): THPM).

*Benzyl 6-methyl-2-oxo-4-p-tolyl-1,2,3,4-tetrahydropyrimidine-5-carboxylate (**1k**)*

Synthesis and the structural of this compound have been reported previously.[32]

*Benzyl 6-methyl-2-oxo-4-(2-hydroxyphenyl)-1,2,3,4-tetrahydropyrimidine-5-carboxylate (**1l**).*

White precipitates. Yield: 51%. M.p. 181-182 °C.IR (KBr): 3252, 3121 (N-H, ureide), 2981 (C-H, aliphatic), 1698 (C=O, ester), 1675, 1466 (C=C, aromatic), 1093 (C-O, ester). ^{1}H-NMR (400 MHz, (D_6)DMSO): 9.18 (s, H-N(1): ureide), 7.64 (s, H-N(3): ureide), 7.43-6.72 (m, H-C: -$CH_2C_6H_5$, C_6H_4OH), 5.53 (s: H-O), 5.23 (d, ^3J = 12.8, H-C(a): $CH_aC_5H_6$), 5.18 (d, ^3J = 12.8, H-C(b): $CH_bC_5H_6$), 4.53 (d, ^3J = 2.8, H-C(4): THPM), 2.30 (s, CH_3 -C(6): THPM).

*General procedure for the synthesis of 6-methyl-2-oxo-4-aryl-1,2,3,4-tetrahydropyrimidine-5-carboxylic acids (**2a-l**)*

A mixture of 6-methyl-2-oxo-4-aryl-1,2,3,4-tetrahydropyrimidine-5-carboxylate esters (**1a-l**) (1 mmol), ammonium formate (10 mmol) and a catalytic amount (0.05 g) of Pd/C (10% w/w) were suspended in 15 mL of dry methanol. The reaction mixture was stirred at room temperature until the completion of the reaction which was monitored by TLC. After completion of the reaction, Pd/C (10% w/w) was separated using filtration. Then, the solvent was completely evaporated under reduced pressure. The solid residue was dissolved in 0.5 M KOH solution (10-15 mL), vigorously stirred, and filtered. The filtrate was acidified by 2M HCl to pH 4-5 and the resulting precipitates of the corresponding 6-methyl-2-oxo-4-aryl-1,2,3,4-tetrahydropyrimidine-5-carboxylic acids (**2a-l**) were collected by filtration and completely dried in electrical oven. General procedure for the preparation of these compounds is provided in Scheme **1**. The obtained compounds were characterized by ^{1}H-NMR, FT-IR, mass spectra and elemental analysis.

*6-Methyl-2-oxo-4-phenyl-1,2,3,4-tetrahydropyrimidine-5-carboxylic acid (**2a**)*

White crystals. Yield 66%. M.p. 212-213°C.FT-IR (KBr): 2500-3200 (O-H, acid), 3225.36 (N-H, ureide), 3102.90 (C-H, aromatic), 2939.95 (C-H, aliphatic), 1702.84 (C=O, acid), 1644.98 (C=O, ureide), 1490.10, 1424.17 (C=C, aromatic), 1230.36 (C-O, acid). ^{1}H-NMR (400 MHz, (D_6)DMSO): 11.81 (brs, COOH), 9.02 (s, H-N(3): ureide), 7.61 (s, H-N(1): ureide), 7.25 (t, ^3J(H,H,H) = 6.6, H-C(3), H-C(4), H-C(5):C_6H_5), 7.17 (d, ^3J(H,H) = 6.4, H-C(2), H-C(6): C_6H_5), 5.04 (d, ^3J = 3.1, H-C(4): THPM), 2.16 (s, CH_3-C(6): THPM). Mass m/z (%): 231.10 (M-1). Anal. Calc. for $C_{12}H_{12}N_2O_3$ (232.24): C 62.06, H 5.21, N 12.06; found: C 61.78, H 5.32, N 11.81.

*6-Methyl-2-oxo-4-(4-(dimethylaminophenyl)-1,2,3,4-tetrahydropyrimidine-5-carboxylic acid (**2b**)*

Pale yellow crystals. Yield 62%. M.p. 237–238°C.FT-IR (KBr): 2500-3200 (O-H, acid), 3222.47, 3099.05 (N-H, ureide), 2929.34 (C-H, aromatic), 2837.85 (C-H, aliphatic), 1700.91 (C=O, acid), 1645.95 (C=O, ureide), 1617.02, 1463.71 (C=C, aromatic), 1230.36 (C-O, acid). ^{1}H-NMR (400 MHz, (D_6)DMSO):11.78 (brs, COOH), 8.99 (s, H-N(3): ureide), 7.53 (s, H-N(1): ureide), 7.05 (d, ^3J(H,H) = 8.7, H-C(2) , H-C(6):

C_6H_5), 6.66 (d, ^3J(H,H) = 8.8, H-C(3), H-C(5): C_6H_5), 5.00 (d, ^3J = 6.5, H-C(4): THPM), 2.85 (s, 2 ×CH_3-N: NCH_3), 2.22 (s, CH_3-C(6): THPM). Mass m/z (%): 274.10 (M-1). Anal. Calc. for $C_{14}H_{17}N_3O_3$ (275.31): C 61.08, H 6.22, N 15.26; found: C 60.94, H 6.31,N 15.11.

*6-Methyl-2-oxo-4-(4-aminophenyl)-1,2,3,4-tetrahydropyrimidine-5-carboxylic acid (**2c**)*

Pale yellow crystals. Yield 20%. M.p. 209 – 210°C.FT-IR (KBr): 2500-3300 (O-H, acid), 3396.99 (N-H, amine), 3226.33, 3102.90 (N-H, ureide), 2943.80 (C-H, aromatic), 2884.74 (C-H, aliphatic), 1682.59 (C=O, acid), 1651.73 (C=O, ureide), 1514.81, 1431.89 (C=C, aromatic), 1239.04 (C-O, acid). ^{1}H-NMR (400 MHz, (D_6)DMSO):11.93 (brs, COOH), 9.12 (s, H-N(3): ureide), 8.13 (brs, H-N: NH_2), 7.67 (s, H-N(1): ureide), 7.16 (d, ^3J(H,H) = 8.4, H-C(2), H-C(6): C_6H_5), 6.95 (d, ^3J(H,H) = 8.4, H-C(3), H-C(5): C_6H_5), 5.09 (d, ^3J = 2.8, H-C(4): THPM), 2.29 (s, CH_3-C(6): THPM). Mass m/z (%): 246.10 (M-1). Anal. Calc. for $C_{12}H_{13}N_3O_3$ (247.25): C 58.29. H 5.30, N 16.99; found: C 57.95, H 5.02, N 16.71.

*6-Methyl-2-oxo-4-(furan-2-yl)-1,2,3,4-tetrahydropyrimidine-5-carboxylic acid (**2d**)*

Pale yellow crystals. Yield 15%. M.p. 202°C decomposed. FT-IR (KBr): 2500-3200 (O-H, acid), 3225.36, 3116.40 (N-H, ureide), 2811.70 (C-H, aliphatic), 1701.87 (C=O, acid), 1644.02 (C=O, ureide), shoulder 1409.71 (C=C, aromatic), 1231.33 (C-O, acid).^{1}H-NMR (400 MHz, (D_6)DMSO):11.93 (brs, COOH), 9.14 (s, H-N(3): ureide), 7.71 (s, H-N(1): ureide), 7.56 (d, ^3J = 0.8, H-C(3): furan), 6.36 (t, ^3J = 2.4, H-C(4): furan), 6.08 (d, ^3J = 3.2, H-C(5): furan), 5.16 (d, ^3J = 3.2, H-C(4): THPM), 2.22 (s, CH_3-C(6): THPM). Mass m/z (%): 221.05 (M-1). Anal. Calc. for $C_{10}H_{10}N_2O_4$ (222.20): C 54.05, H 4.54, N 12.61; found: C 54.31, H 4.78, N, 12.45.

*6-Methyl-2-oxo-4-(4-chlorophenyl)-1,2,3,4-tetrahydropyrimidine-5-carboxylic acid (**2e**)*

White crystals. Yield 68%. M.p. 218–219°C.FT-IR (KBr): 2500-3200 (O-H, acid), 3225.36, 3103.87 (N-H, ureide), 2938.02 (C-H, aliphatic), 1700.91 (C=O, acid), 1644.02 (C=O, ureide), 1465.63 (C=C, aromatic), 1229.40 (C-O, acid). ^{1}H-NMR (400 MHz, (D_6)DMSO):11.94 (brs, COOH), 9.16 (s, H-N(3): ureide), 7.73 (s, H-N(1): ureide), 7.39 (d, ^3J(H,H) = 8.4, H-C(3), H-C(5): C_6H_5), 7.26 (d, ^3J(H,H) = 2.8 , H-C(2), H-C(6): C_6H_5), 5.11 (d, ^3J = 2.8, H-C(4): THPM), 2.24 (s, CH_3-C(6): THPM). Mass m/z (%): 265.05 (M-1). Anal. Calc. for $C_{12}H_{11}ClN_2O_3$ (266.68): C 54.05, H 4.16, N 10.50; found: C 54.33, H 4.25, N 10.61.

*6-Methyl-2-oxo-4-(4-fluorophenyl)-1,2,3,4-tetrahydropyrimidine-5-carboxylic acid (**2f**)*

White crystals. Yield 57%. M.p. 212–213°C.FT-IR (KBr): 2500-3200 (O-H, acid), 3226.33, 3105.80 (N-H, ureide), 2938.02 (C-H, aliphatic), 1703.80 (C=O, acid), 1644.98 (C=O, ureide), 1604.48, 1509.03 (C=C, aromatic), 1230.36 (C-O, acid). ^{1}H-NMR (400 MHz, (D_6)DMSO): 12.24 (brs, COOH), 9.11 (s, H-N(3): ureide), 7.68 (s, H-N(1): ureide), 7.25-7.28 (m, H-C(3), H-C(5): C_6H_5), 7.15-7.17 (m, H-C(2), H-C(6): C_6H_5), 5.12 (d, ^3J = 3.2, H-C(4): THPM), 2.24 (s, CH_3-C(6): THPM). Mass m/z (%): 249.05 (M-1). Anal. Calc. for $C_{12}H_{11}FN_2O_3$ (250.23): C 57.60, H 4.43, N 11.20; found: C 57.32, H 4.49, N 11.03.

*6-Methyl-2-oxo-4-(2-chlorophenyl)-1,2,3,4-tetrahydropyrimidine-5-carboxylic acid (**2g**)*

White crystals. Yield 46%.M.p. 247–248°C.FT-IR (KBr): 2500-3200 (O-H, acid), 3224.40, 3103.87 (N-H, ureide), 2951.52 (C-H, aliphatic), 1703.80 (C=O, acid), 1644.02 (C=O, ureide), 1469.49, 1423.10 (C=C, aromatic), 1230.36 (C-O, acid). ^{1}H-NMR (400 MHz, (D_6)DMSO):11.82 (brs, COOH), 9.18 (s, H-N(3): ureide), 7.60 (s, H-N(1): ureide), 7.27-7.42 (m, H-C:C_6H_5), 5.57-5.58 (m, H-C(4): THPM), 2.30 (s, CH_3-C(6): THPM). Mass m/z (%): 265.05 (M-1). Anal. Calc. for $C_{12}H_{11}ClN_2O_3$ (266.68): C 54.05, H 4.16, N10.50; found: C 54.31, H 4.28, N 10.35.

*(E) 6-Methyl-2-oxo-4-styryl-1,2,3,4-tetrahydropyrimidine-5-carboxylic acid (**2h**)*

White crystals. Yield 20%.M.p. 214-215°C.FT-IR (KBr): 2500-3300 (O-H, acid), 3235.00, 3106.76 (N-H, ureide), 3027.69 (C-H, aromatic), 2928.38, 2860.88 (C-H, aliphatic), 1686.44 (C=O, acid), 1657.52 (C=O, ureide), 1625.66 (C=C, alkene), 1620.74, 1599.66 (C=C, aromatic), 1272.79 (C-O, acid). ^{1}H-NMR (400 MHz, (D_6)DMSO):11.77 (brs, COOH), 8.85 (s, H-N(3): ureide), 7.37 (s, H-N(1): ureide), 7.16-7.20 (m, H-C(3), H-C(4), H-C(5): C_6H_5,H-C(a), H-C(b): alkene), 7.09-7.10 (m, H-C(2), H-C(6): C_6H_5), 3.99-4.03 (m, H-C(4): THPM), 2.09 (s, CH_3-C(6): THPM). Mass m/z (%): 257.10 (M-1). Anal. Calc. for $C_{14}H_{14}N_2O_3$ (258.28): C 65.11, H 5.46, N 10.85; found: C 64.79, H 5.78, N 10.63.

*6-Methyl-2-oxo-4-(3-aminophenyl)-1,2,3,4-tetrahydropyrimidine-5- carboxylic acid (**2i**)*

Yellow crystals. Yield 23%.M.p. 223–224°C.FT-IR (KBr): 2500-3500 (O-H, acid), 3323.71 (N-H, amine), 3109.65, 3108.69 (N-H, ureide), 2976.59, 2909.09 (C-H, aromatic), 2878.24, 2850.27 (C-H, aliphatic), 1708.62 (C=O, acid), 1643.05 (C=O, ureide), 1605.45, 1569.77 (C=C, aromatic), 1346.07 (C-N, amine), 1093.44 (C-O, acid). ^{1}H-NMR (400 MHz, (D_6)DMSO):11.60 (brs, COOH), 9.75 (s, H-N(3): ureide), 9.18 (s, H-N(1): ureide), 8.48 (brs, H-N: NH_2), 7.61-7.62 (m, H-C(5): C_6H_5), 7.59-7.60 (m, H-C(6): C_6H_5), 7.56 (brs, H-C(4): C_6H_5), 7.54 (brs, H-C(2): C_6H_5), 4.99 (s, H-C(4): THPM), 2.29(s, CH_3-C(6): THPM). Mass m/z (%): 246.10 (M-1). Anal. Calc. for $C_{12}H_{13}N_3O_3$ (247.25): C 58.29, H 5.30, N16.99; found: C 58.02, H 5.16, N 16.73.

*6-Methyl-2-oxo-4-(thiophen-2-yl)-1,2,3,4-tetrahydropyrimidine-5-carboxylic acid (**2j**)*

Yellow crystals. Yield 25%. M.p. 213–215°C.FT-IR (KBr): 2500-3500 (O-H, acid), 3396.99, 3226.33 (N-H, ureide), 3102.90 (C-H, aromatic), 2943.80, 2892.74 (C-H, aliphatic), 1686.44 (C=O, acid), 1657.52 (C=O, ureide), 1625.66, 1620.14, 1599.66 (C=C, aromatic), 1272.79 (C-O, acid). ^{1}H-NMR (400 MHz, (D_6)DMSO):11.93 (brs, COOH), 9.40 (s, H-N(3): ureide), 8.09 (s, H-N(1): ureide), 7.84 (d, ^3J = 0.8, H-C(3): thiophen), 6.63 (dd, ^3J = 1.2,^3J = 3.2, H-C(4): thiophen), 6.37 (d, ^3J = 3.2, H-C(5): thiophen), 5.22 (d, ^3J = 3.2, H-C(4): THPM), 2.22 (s, CH_3-C(6): THPM). Mass m/z (%): 237.05 (M-1). Anal. Calc. for $C_{10}H_{10}N_2O_3S$ (238.27): C 50.41, H 4.23, N 11.76, S 13.46; found: C 50.58, H 4.45, N 12.04, S 13.59.

*6-Methyl-2-oxo-4-p-tolyl-1,2,3,4-tetrahydropyrimidine-5-carboxylic acid (**2k**)*

Synthesis and the structural features of this compound have been reported previously.[32]

*6-Methyl-2-oxo-4-(2-hydroxyphenyl)-1,2,3,4-tetrahydropyrimidine-5-carboxylic acid (**2l**)*

White crystals. Yield 20%. M.p. 235–237°C.FT-IR (KBr): 2600-3500 (O-H, acid), 3071.08 (C-H, aromatic), 2935.13 (C-H, aliphatic), 1647.88 (C=O, acid), 1587.13 (C=O, ureide), 1490.70, 1456.96 (C=C, aromatic), 1230.36 (C-O, acid), 1166.97 (C-O, phenol).^{1}H-NMR (400 MHz, (D_6)DMSO): 11.82 (brs, COOH), 9.18 (s, H-N(3): ureide), 7.60 (s, H-N(1): ureide), 7.27-7.42 (m, H-C: C_6H_5), 6.12 (s, H-O: OH), 5.58 (d,^3J = 2.8, H-C(4): THMP), 2.30 (s, CH_3-C(6): THPM). Mass m/z (%): 247.15 (M-1). Anal. Calc. for $C_{12}H_{12}N_2O_4$ (248.24): C 58.06, H 4.87, N 11.29; found: C 58.30, H 5.05, N 11.48.

Biological assay

Inhibition of the HIV-1 entry by the prepared compounds was investigated. **BMS-806**[33] as the control HIV-1 surface glycoprotein inhibitor was used in the experiments. Synthesized compounds were dissolved in dimethyl sulfoxide (DMSO) at different concentrations. DMSO with the final concentration of 1% V/V (1 mL DMSO in 100 mL H_2O) was considered as the negative solvent control. DMSO plus MT-2 (human lymphocyte) cells and virus were used to normalize the solvent effect.[34] BMS-806 (200 mM) was dissolved in DMSO and kept at -20°C. All tests were performed in triplicate.

Inhibition of HIV-1 single-cycle infection

Human embryonic kidney (HEK) and MT-2 cells were obtained from National Cell Bank of Iran. MT-2 cells were produced by co-culturing normal human cord leukocytes with leukemic T-cells from a patient with adult T-cell leukemia. To measure the inhibition effect, HEK 293T cells were cultured in RPMI 1640 and DMEM (Dulbecco's modified Eagle's medium) containing 15% L-FBS (Fetal Bovine Serum), 100 U/mL of penicillin, and 100 µg/mL of streptomycin.[35] In the step of transfection into HEK cells, HEPES (4-(2-hydroxyethyl)-1-piperazine ethane sulfonic acid) was added and finally the cells were incubated at 37 °C under 5% CO_2.

To produce the SCR HIV-1 virions, pMD2G, pmzNL4-3 and pSPAX2 plasmids were used. These plasmids were co-transfected into HEK 293T cells in 6-well plates (5×105 cells/well) in certain proportion using PolyFect reagent (Qiagen) according to the suggested method by Qiagen. Supernatants of the transfected cells were harvested after 24, 48 and 72 h after infection and fresh medium was added to the culture wells. Mediums containing viruses were mixed together and stored at -70°C after filtration with 0.22 µm filters.[36] Final centrifugation on the filtrate at 60,000 g was performed for 2 h at 4°C. The supernatant was taken out and the virions pellet was shaken gently overnight in 1/30 volume of RPMI 1640 at 4 ºC. SCR HIV-1 virions were produced in 24-well

plates to generate viruses for measuring the rate of production and maturation. 70×103 HEK 293T cells were used for producing SCR HIV-1 virions by 400 ng of plasmid. Transfection was carried out in the presence of 4 µL of PolyFect reagent. Volume of transfection was 300 µL and the volume of the added DNA complex was 120 µL. When transfection was complete, 800 µL of the complete medium containing the synthesized compounds was added to the cells. The culture medium containing the virus was collected 48 h after transfection and the amount of the purified virus was measured using p24 ELISA assay kit (Cell Biolabs).[37]

Cytotoxicity assay

The toxicity of compounds for the target cell (Hela) was assayed using XTT (sodium 3-[1 (phenylaminocarbonyl)-3,4-tetrazolium]-bis(4-methoxy-6-nitro)benzene sulfonic acid) (Roche, Germany) as described previously. The replication assay plates were directly subjected to XTT assay after analysis of supernatant for P24 load. Before addition of XTT, the medium was aspirated and replaced with phosphate-buffered saline (PBS). The XTT solution was prepared and added to the wells according to the user manual. Cell was then incubated for an additional 2 h to allow the formazan production. The optical densities were measured with ELISA reader at test and reference wave lengths of 492 nm and 690 nm, respectively.

In Silico studies

In silico calculation of physicochemical parameters and ADMET prediction

Lipinski's ''Rule of five'' and the physicochemical properties of the designed derivatives were calculated using online Osiris property explorer[29] and MolinspirationWebME Editor1.16.[38] Some of these properties are CLogP, LogS, molecular weight (MW), drug-likeness, number of hydrogen bond donors (HBD), number of hydrogen bond acceptors (HBA), number of rotatable bonds (nROTB) and drug score. Topological polar surface area (TPSA) was assessed using MolinspirationWebME Editor1.16. Percentage of absorption (%ABS) was calculated by %ABS = 109-(0.345×TPSA) formula.[28] In silico toxicity risks, i.e. mutagenicity, tumorigenicity, irritant effect, reproductive effect of synthesized compounds were also predicted using the following online bioinformatics tools.[29]

Molecular docking studies

Molecular docking studies were carried out by AutoDock version 4.2.[39] The three-dimensional (3D) protein structure of gp41 (PDB ID: 1AIK), determined by X-ray crystallography, was retrieved from the RCSB Protein Data Bank (http://www.rcsb.org/pdb/home/home.do). Then the protein was corrected by removing extra crystallized water molecules using Accelrys discovery studio visualizer 4.0 (DS Visualizer,

Accelrys Software Inc. San Diego CA USA 2014) and adding polar hydrogens and charges by Autodock software.[40] Protonation step corrects the ionization and tautomeric states of residues and thus modifies the total Kollman charges on the protein structure. All two-dimensional (2D) structures of the ligands were drawn by ChemDraw program (ChemDraw Ultra10.0, Cambridge soft). Each structure was energy minimized by MM+ force field and PM3 semi-empirical techniques in HyperChem8 software. Then, the partial charges of atoms were calculated using Gasteiger-Marsili procedure. Non-polar hydrogens of compounds were merged, rotatable bonds were assigned and finally the molecules were saved as pdbqt file format using AutoDockTools version 1.5.6 RC3 (http://mgltools.scripps.edu). The resulting protein structure was used as an input for the AutoGrid program. AutoGrid performs pre-calculated atomic affinity grid maps for each atom type in the ligand, plus an electrostatics map and a separate desolvation map presented in the substrate molecule. All maps were calculated with 0.375 Å spacing between grid points. Grid center was centered on Cα atom of Lys574 residue with coordinates x=24.00, y=21.82, z=23.82, obtained by the Acceryls discovery studio visualizer 4.0. The location and size of the grid was set in a way to contain not only the active site but also considerable portions of the surrounding surface. For this purpose, box was set at 60 × 60 × 60 Å. Each docked system was done by 150 runs of the AutoDock search by the Lamarckian genetic algorithm (LGA). The factors for LGA were defined as follows: a maximum number of 5,000,000 energy evaluations; a maximum number of generations of 27,000; mutation and crossover rates of 0.02 and 0.8, respectively. Lastly, conformation of the lowest predicted binding free energy of the most occurring binding modes in the gp41 active pocket was selected. Graphic manipulations and visualizations were done by Autodock Tools or Accelrys discovery studio visualizer 4.0 software.

References

[1] E. O. Freed, M. A. Martin,'The role of human immunodeficiency virus type 1 envelope glycoproteins in virus infection',*J. Biol. Chem,***1995**, *270*, 23883-23886.

[2] E. Krambovitis, F. Porichis, A. D. Spandidos,'HIV entry inhibitors: a new generation of antiretroviral drugs', *Acta. Pharmacologica. Sinica.***2005**, *26*,1165-1173.

[3] S. E. Schneider, B. L. Bray, C. J. Mader, P. E. Friedrich, M. W. Anderson, T. S. Taylor, N. Boshernitzan, T. E. Niemi, B. C. Fulcher, S. R. Whight, J. M. White, R. J. Greene, L. E. Stoltenberg, M. Lichty, 'Development of HIV fusion inhibitors', *J. Pept. Sci,***2005**, *11*, 744-753.

[4] S. A. Gallo, A. Puri, R. Blumenthal, 'HIV-1 gp41 six-helix bundle formation occurs rapidly after the engagement of gp120 by CXCR4 in the HIV-1 Env-mediated fusion process',*Biochemistry*, **2001**,*40*,12231-12236.

[5] M. Gochin, L. R. Whitby, A. H. Phillips, D. L. Boger,'NMR-assisted computational studies of peptidomimetic inhibitors bound in the hydrophobic pocket of HIV-1 glycoprotein 41', J*. Comput. Aided. Mol. Des,***2013**, *27*,569-582.

[6] D. C. Chan, C. T. Chutkowski, P. S. Kim, 'Evidence that a prominent cavity in the coiled coil of HIV type 1 gp41 is an attractive drug target', *Proc. Natl. Acad. Sci. USA,***1998**, *95*,15613-15617.

[7] S. Jiang, K. Lin, L. Zhang, A. K. J. Debnath, 'A screening assay for antiviral compounds targeted to the HIV-1 gp41 core structure using a conformation-specific monoclonal antibody', *Virol. Meth,***1999**, *80*, 85-96.

[8] S. Liu, S. Wu, S. Jiang, 'HIV entry inhibitors targeting gp41: from polypeptides to small-molecule compounds', *Curr. Pharm. Des,***2007**,*13*,143-162.

[9] G. Frey, S. Rits-Volloch, X. Q. Zhang, R. T. Schooley, B. Chen, S. C. Harrison, 'Small molecules that bind the inner core of gp41 and inhibit HIV envelope-mediated fusion', *PNAS,* **2006**,*103*, 13938-13943.

[10] C. Teixeira, F. Barbault, J. Rebehmed, K. Liu, L. Xie, H. Lu, S. Jiang, B. T. Fan, F. Maurel, 'Molecular modeling studies of N-substituted pyrrole Derivatives-Potential HIV-1 gp41 inhibitors', *Bioorg. Med. Chem,***2008**,*16*,3039-3048.

[11] K. Liu, H. Lu, L. Hou, Z. Qi, C. Teixeira, F. Barbault, B. T. Fan, S. Liu, S. Jiang, L. Xie, 'Design, Synthesis, and Biological Evaluation of N-Carboxyphenylpyrrole Derivatives as Potent HIV Fusion Inhibitors Targeting gp41', J*. Med. Chem*,**2008**,*51*,7843-7854.

[12] A. R. Katritzky, S. R. Tala, H. Lu, A. V. Vakulenko, Q. Y. Chen, J. Sivapackiam, K. Pandya, S. Jiang, A. K. Debnath, 'Design, Synthesis, and Structure-Activity Relationship of a Novel Series of 2-Aryl 5-(4-Oxo-3-phenethyl-2-thioxothiazolidinylidenemethyl)furans as HIV-1 Entry Inhibitors', *J. Med. Chem*,**2009**, *52*,7631-7639.

[13] K. D. Stewart, J. R. Huth, T. I. Ng, K. McDaniel, R. N. Hutchinson, V. S. Stoll, R. R. Mendoza, E. D. Matayoshi, R. Carrick, H. M. Moa, J. Severin, K. Walter, P. L. Richardson, L. W. Barrett, R. Meadows, S. Anderson, W. Kohlbrenner, C. Maring, D. J. Kempf, A. Molla, E. T. Olejniczak, 'Non-peptide entry inhibitors of HIV-1 that target the gp41 coiled coil pocket', *Bioorg. Med. Chem. Lett*,**2010**, *20*,612-617.

[14] G. Zhou, D. Wua, E. Hermel, E. Balogh, M. Gochin, 'Design, synthesis, and evaluation of indole compounds as novel inhibitors targeting gp41', *Bioorg. Med. Chem. Lett*,**2010**, *20*,1500-1503.

[15] Y. Wang, H. Lu, Q. Zhu, S. Jiang, Y. Liao, 'Structure-based design, synthesis and biological evaluation of new N-carboxyphenylpyrrole derivatives as HIV fusion inhibitors targeting gp41', *Bioorg. Med. Chem. Lett*,**2010**, *20*,189-192.

[16] X. Y. He, P. Zou, J. Qiu, L. Hou, S. Jiang, S. Liu, L. Xie, 'Design, synthesis and biological evaluation of 3-substituted 2,5-dimethyl-N-(3-(1H-tetrazol-5-yl)phenyl)pyrroles as novel potential HIV-1 gp41 inhibitors', *Bioorg. Med. Chem*,**2011**,*19*, 6726-6734.

[17] G. Zhou, D. Wu, B. Snyder, R. G. Ptak, H. Kaur, M. Gochin, Development of indole compounds as small molecule fusion inhibitors targeting HIV-1 glycoprotein-41', *J. Med. Chem*,**2011**, *54*,7220-7231.

[18] S. Jiang, S. R. Tala, H. Lu, P. Zou, I. Avan, T. S. Ibrahim, N. E. Abo-Dya, A. Abdelmajeid, A. K. Debnath, A. R. Katritzky, 'Design, synthesis, and biological activity of a novel series of 2,5-disubstituted furans/pyrroles as HIV-1 fusion inhibitors targeting gp41', *Bioorg. Med. Chem. Lett*,**2011**, *21*,6895-6898.

[19] K. D. Stewart, K. Steffy, K. Harris, J. E. Harlan, V. S. Stoll, J. R. Huth, K. A. Walter, E. Gramling-Evans, R. R. Mendoza, J. M. Severin, P. L. Richardson, L. W. Barrett, E. D. Matayoshi, K. M. Swift, S. F. Betz, S. W. Muchmore, D. J. Kempf, A. Molla, 'Design and characterization of an engineered gp41 protein from human immunodeficiency virus-1 as a tool for drug discovery', *J. Comput. Aided. Mol. Des*,**2007**, *21*,121-130.

[20] S. Sepehri, S. Gharagani, L. Saghaie, M. R. Aghasadeghi, A. Fassihi, 'QSAR and docking studies of some 1,2,3,4-tetrahydropyrimidines: evaluation of gp41 as possible target for anti-HIV-1 activity', *Med. Chem. Res*,**2015**,*24*,1707-1724.

[21] R. J. Clemens, J. A. Hyatt, 'Acetoacetylation with 2,2,6-trimethyl-4H-1,3-dioxin-4-one: a convenient alternative to diketene', *J. Org. Chem*,**1985**,*50*,2431-2433.

[22] H. H. F. Refsgaard, B. F. Jensen, P. B. Brockhoff, S. B. Padkjaer, M. Guldbrandt, M. S. Chistensen,'*In silico* prediction of membrane permeability from calculated molecular parameters',*J. Med. Chem*,**2005**, *48*,805-811.

[23] D. F. Veber, S. R. Johnson, H. Y. Cheng, B. R. Smith, K. W. Ward, K. D. Kapple, 'Molecular properties that influences the oral bioavailability of drug candidates', *J. Med. Chem*,**2002**, *45*,2615-2623.

[24] C. A. Lipinski, F. Lombardo, B. W. Dominy, P. J. Feeney, 'Experimental and computational approaches to estimate solubility and permeability in drug discovery and development setting', *Adv. Drug. Deliv. Rev*,**1997**, *23*,23-25.

[25] G. Vistoli, A. Pedretti, B. Testa, 'Assessing drug-likeness-what are we missing?', *Drug. Discov. Today*,**2008**, *13*,285-294.

[26] P. Ertl, B. Rohde, P. Selzer, 'Fast calculation of molecular polar surface area as a sum of fragment-based contributions and its application to the prediction of drug transport properties', *J. Med. Chem*,**2000**, *43*,3714-3717.

[27] D. E. Clark, S. D. Pickett, 'Computational methods for the prediction of 'drug-likeness', *Drug. Discov. Today*,**2000**, *5*,49-58.

[28] Y. Zhao, M. H. Abraham, J. Lee, A. Hersey, N. C. Luscombe, G. Beck, B. Sherborne, I. Cooper, 'Rate-limited steps of human oral absorption and QSAR studies', *Pharm. Res*,**2002**, *19*,1446-1457.

[29] Http://www.Organic-chemistry.org/prog/peo/, accessed in May 2016.

[30] R. P. Sellers, L. D. Alexander, V. A. Johnson, C. C. Lin, J. Savage, R. Corral, J. Moss, T. S. Sluqocki, E. K. Singh, M. R. Davis, S. Ravula, J. E. Spicer, J. L. Oelrich, A. Thornquist, C. M. Pan, S. R. McAlpine, 'Design and synthesis of Hsp90 inhibitors: exploring the SAR of Sansalvamide A derivatives', *Bioorg. Med. Chem. Lett*,**2010**, *18*,6822-6856.

[31] C. Teixeira, N. Serradji, F. Maurel, F. Barbault, ' Docking and 3D-QSAR studies of BMS-806 analogs as HIV-1 gp120 entry inhibitors', *Eur. J. Med. Chem.***2009**,44,3524-3532.

[32] B. Desai, D. Dallinger, C. O. Kappe, 'Microwave-assisted solution phase synthesis of dihydropyrimidine C5 amides and esters', *Tetrahedron*,**2006**,*62*,4651-4664.

[33] W. C. Olson, P. J. Maddon, 'Resistance to HIV-1 entry inhibitors', *Curr. Drug. Targets. Infect. Disord*,**2003**, *3*, 283-294.

[34] M. Peeters, R. Vincent, J. L. Perret, M. Lasky, D. Patrel, F. Liegeois, V. Courgnaud, R. Seng, T. Matton, S. Molinier, E. Delaporte, 'Evidence for differences in MT-2 cell tropism according to genetic

subtypes of HIV-1: syncytium-inducing variants seem rate among subtype C HIV-1 viruses', *J. Acquir. Immune. Defic. Syndr*,**1998**, *20*, 115-12.

[35] A. Adachi, H. E. Gendelman, S. Koenig, T. Folks, R. Willey, A. Rabson, 'Production of acquired immunodeficiency syndrome-associated retrovirus in human and nonhuman cells transfected with an infectious molecular clone', *J. Virol*,**1986**,*59*,284-291.

[36] E. M. Campbell, O. Perez, M. Melar, T. J. Hope, 'Labeling HIV-1 virions with two fluorescent proteins allows identification of virions that have productively entered the target cell', *Virology*,**2007**, *360*,286-293.

[37] R. Zabihollahi, S. M. Sadat, R. Vahabpour, M. R. Aghasadeghi, A. Memarnejadian, T. Ghazanfari, M. Salehi, A. Rezaei, k. Azadmanesh, 'Development of single-cycle replicable human immunodeficiency virus 1 mutants', *Acta. Virol*,**2011**, *55*,15-22.

[38] Http://www.Molinspiration.com, accessed in May 2016.

[39] G. M. Morris, R. Huey, W. Lindstrom, M. F. Sanner, R. K. Belew, D. S. Goodsell, A. J. J. Olson, 'AutoDock4 and AutoDockTools4: Automated docking with selective receptor flexibility', *Comput. Chem*,**2009**, *30*,2785-2791.

[40] G. M. Morris, R. Huey, A. J. Olson, 'Using AutoDock for ligand–receptor docking. Current Protocols in Bioinformatics', *Curr. Protoc. Bioinformatics*,**2008**, Chapter 8, Unit 8, 14.